

Multimodal Study of Secondary Interactions in Cp*Ir Complexes of Imidazolylphosphines Bearing an NH Group

Douglas B. Grotjahn,^{*,†} John E. Kraus,[†] Hani Amouri,[‡] Marie-Noelle Rager,[§]
Andrew L. Cooksy,[†] Amy J. Arita,[†] Sara A. Cortes-Llamas,^{†,⊥} Arthur A. Mallari,[†]
Antonio G. DiPasquale,[#] Curtis E. Moore,[#] Louise M. Liable-Sands,^{||,#}
James D. Golen,^{||,#} Lev N. Zakharov,[#] and Arnold L. Rheingold[#]

Department of Chemistry and Biochemistry, 5500 Campanile Drive, San Diego State University, San Diego, California 92182-1030, Institut Parisien de Chimie Moléculaire, UMR CNRS 7201, Université Pierre et Marie Curie-Paris 6, 4 place Jussieu, case 42, 75252 Paris Cedex 05, France, NMR Facilities of Ecole Nationale Supérieure de Chimie de Paris, 11 Rue Pierre et Marie Curie, 75231 Paris Cedex 05, France, Department of Chemistry, Widener University, One University Place, Chester, Pennsylvania 19013, Department of Chemistry and Biochemistry, University of Massachusetts Dartmouth, North Dartmouth, Massachusetts 02747, and Department of Chemistry and Biochemistry, University of California, San Diego, La Jolla, California 92093-0385

Received August 7, 2009; E-mail: grotjahn@chemistry.sdsu.edu

Abstract: Hydrogen bonding phenomena are explored using a combination of X-ray diffraction, NMR and IR spectroscopy, and DFT calculations. Three imidazolylphosphines R₂PImH (ImH = imidazol-2-yl, R = *t*-butyl, *i*-propyl, phenyl, **1a–1c**) and control phosphine (*i*-Pr)₂PhP (**1d**) lacking an imidazole were used to make a series of complexes of the form Cp*Ir(L₁)(L₂)(phosphine). In addition, in order to suppress intermolecular interactions with either imidazole nitrogen, **1e**, a di(isopropyl)imidazolyl analogue of **1b** was made along with its doubly ¹⁵N-labeled isotopomer to explore bonding interactions at each imidazole nitrogen. A modest enhancement of transfer hydrogenation rate was seen when an imidazolylphosphine ligand **1b** was used. Dichloro complexes (L₁ = L₂ = Cl, **2a–2c,2e**) showed intramolecular hydrogen bonding as revealed by four X-ray structures and various NMR and IR data. Significantly, hydride chloride complexes [L₁ = H, L₂ = Cl, **3a–3c** and **3e-(¹⁵N)₂**] showed stronger hydrogen bonding to chloride than hydride, though the solid-state structure of **3b** evinced intramolecular Ir–H···H–N bonding reinforced by intermolecular N···H–N bonding between unhindered imidazoles. These results are compared to literature examples, which show variations in preferred hydrogen bonding to hydride, halide, CO, and NO ligands. Surprising differences were seen between the dichloro complex **2b** with isopropyl groups on phosphorus, which appeared to exist as a mixture of two conformers, and related complex **2a** with *tert*-butyl groups on phosphorus, which exists in chlorinated solvents as a mixture of conformer **2a-endo** and chelate **5a-Cl**, the product of ionization of one chloride ligand. This difference became apparent only through a series of experiments, especially ¹⁵N chemical shift data from 2D ¹H–¹⁵N correlation. The results highlight the difficulty of characterizing hemilabile, bifunctional complexes and the importance of innocent ligand substituents in determining structure and dynamics.

Introduction

Traditional means of fine-tuning the reactivity of organometallic catalysts include changing ligand size or electronic properties or the oxidation state or charge of the metal. In contrast, a growing body of research^{1–7} highlights the benefits of using secondary interactions provided by a ligand functional group or groups outside the metal coordination sphere. This approach to enhancing reactivity resembles features of Nature's metalloenzymes, many of which use multiple proton transfer

or hydrogen bonding interactions to create exquisite catalysts. Our research group has used phosphine ligands capable of proton transfer or hydrogen bonding to speed anti-Markovnikov alkyne hydration by more than 1000 times⁸ and alkene isomerization by more than 10 000 times.⁹ The ligands used in these cases contained a heterocyclic nitrogen. In the course of structural

[†] San Diego State University.

[‡] Université Pierre et Marie Curie-Paris 6.

[§] Ecole Nationale Supérieure de Chimie de Paris.

[⊥] Fulbright Scholar on leave from Universidad de Guadalajara to SDSU.

^{||} Widener University.

[#] University of Massachusetts Dartmouth.

[#] University of California, San Diego.

(1) van den Beuken, E. K.; Feringa, B. L. *Tetrahedron* **1998**, *54*, 12985–13011.

(2) Rowlands, G. J. *Tetrahedron* **2001**, *57*, 1865–1882.

(3) Clapham, S. E.; Hadzovic, A.; Morris, R. H. *Coord. Chem. Rev.* **2004**, *248*, 2201–2237.

(4) Grotjahn, D. B. *Chem.—Eur. J.* **2005**, *11*, 7146–7153.

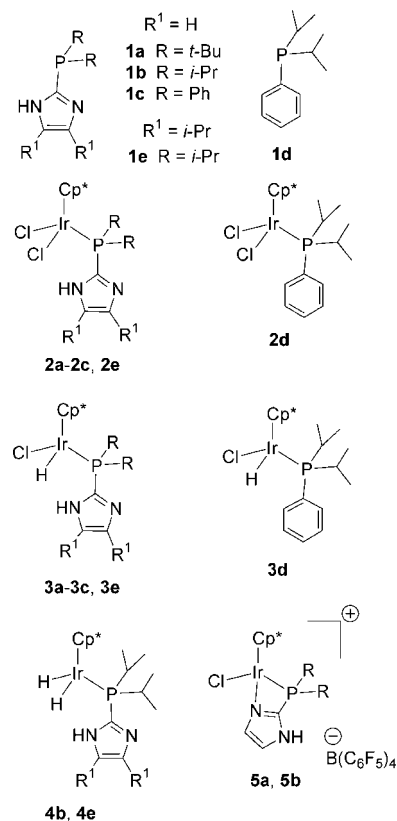
(5) Ikariya, T.; Murata, K.; Noyori, R. *Org. Biomol. Chem.* **2006**, *4*, 393–406.

(6) Natale, D.; Mareque-Rivas, J. C. *Chem. Commun.* **2008**, 425–437.

(7) Das, S.; Brudvig, G. W.; Crabtree, R. H. *Chem. Commun.* **2008**, 413–424.

and mechanistic studies,¹⁰ we have provided conclusive evidence in key catalytic intermediates of alkyne hydration for the ability of a basic heterocyclic nitrogen to accept a hydrogen bond¹¹ and for the ability of a protonated pyridine nitrogen to donate a hydrogen bond.^{12,13} In contrast, we have also shown on square-planar Pt(II) that a neutral heterocyclic NH can donate a hydrogen bond to an oxygenated ligand.¹⁴ In this work, we investigate secondary interactions on a completely different metal and ligand set, octahedral Cp*Ir(III) bearing hydride and chloride ligands. There are several literature studies of hydrogen bonding to late transition metal complexes (H)(X)ML_n, where X = halide: in one series of papers, intermolecular approach of O–H and N–H bonds appears to occur at a chloride ligand rather than a hydride,^{15,16} whereas in another study, intramolecular approach of an O–H or N–H bond to hydride is favored over approach to chloride, bromide, or iodide.¹⁷ In still other hydride complexes, hydrogen bonding to CO or NO ligands rather than to hydride has been seen.^{15,18–20} Thus, it is not entirely clear what will be the preferred bonding site in a given system, nor why one system would prefer one interaction over another. Here, through a combination of spectroscopic and X-ray diffraction data, we demonstrate stronger intramolecular hydrogen bonding on Cp*Ir complexes to the chloride than to the hydride, rather than dihydrogen bonding,^{21–29} and we further probe these interactions through quantum chemical modeling.

Scheme 1. Ligands and Complexes Made in This Study



- (8) (a) Grotjahn, D. B.; Lev, D. A. *J. Am. Chem. Soc.* **2004**, *126*, 12232–12233. For subsequent work, see: (b) Labonne, A.; Kribber, T.; Hintermann, L. *Org. Lett.* **2006**, *8*, 5853–5856. (c) Kribber, T.; Labonne, A.; Hintermann, L. *Synthesis* **2007**, 2809–2818.
- (9) Grotjahn, D. B.; Larsen, C. R.; Gustafson, J. L.; Nair, R.; Sharma, A. *J. Am. Chem. Soc.* **2007**, *129*, 9592–9593.
- (10) Grotjahn, D. B. *Dalton Trans.* **2008**, 6497–6508.
- (11) Grotjahn, D. B.; Miranda-Soto, V.; Kragulj, E. J.; Lev, D. A.; Erdogan, G.; Zeng, X.; Cooksy, A. L. *J. Am. Chem. Soc.* **2008**, *130*, 20–21.
- (12) Grotjahn, D. B.; Kragulj, E. J.; Zeinalipour-Yazdi, C. D.; Miranda-Soto, V.; Lev, D. A.; Cooksy, A. L. *J. Am. Chem. Soc.* **2008**, *130*, 10860–10861.
- (13) Pyridylphosphines have also been used to speed alkyne carboxylation. For mechanistic studies related to this reaction, see: Scriver, A.; Beghetto, V.; Campagna, E.; Zanato, M.; Matteoli, U. *Organometallics* **1998**, *17*, 630–635.
- (14) Grotjahn, D. B.; Gong, Y.; DiPasquale, A. G.; Zakharov, L. N.; Rheingold, A. L. *Organometallics* **2006**, *25*, 5693–5695.
- (15) Belkova, N. V.; Shubina, E. S.; Gutsul, E. I.; Epstein, L. M.; Eremenko, I. L.; Nefedov, S. E. *J. Organomet. Chem.* **2000**, *610*, 58–70.
- (16) Yandulov, D. V.; Caulton, K. G.; Belkova, N. V.; Shubina, E. S.; Epstein, L. M.; Khoroshun, D. V.; Musaev, D. G.; Morokuma, K. *J. Am. Chem. Soc.* **1998**, *120*, 12553.
- (17) Peris, E.; Lee, J.; Jesse, C.; Rambo, J. R.; Eisenstein, O.; Crabtree, R. H. *J. Am. Chem. Soc.* **1995**, *117*, 3485–3491.
- (18) Belkova, N. V.; Ionidis, A. V.; Epstein, L. M.; Shubina, E. S.; Gruendemann, S.; Golubev, N. S.; Limbach, H.-H. *Eur. J. Inorg. Chem.* **2001**, 1753–1761.
- (19) Belkova, N. V.; Besora, M.; Epstein, L. M.; Lledos, A.; Maseras, F.; Shubina, E. S. *J. Am. Chem. Soc.* **2003**, *125*, 7715–7725.
- (20) Belkova, N. V.; Epstein, L. M.; Shubina, E. S. *ARKIVOC* **2008**, 120–138.
- (21) Crabtree, R. H.; Siegbahn, P. E. M.; Eisenstein, O.; Rheingold, A. L.; Koetzle, T. F. *Acc. Chem. Res.* **1996**, *29*, 348–354.
- (22) Custelcean, R.; Jackson, J. E. *Chem. Rev.* **2001**, *101*, 1963–1980.
- (23) Epstein, L. M.; Shubina, E. S. *Coord. Chem. Rev.* **2002**, *231*, 165–181.
- (24) Bakhmutov, V. I. *Eur. J. Inorg. Chem.* **2005**, 245–255.
- (25) *Recent Advances in Hydride Chemistry*; Peruzzini, M., Poli, R., Eds.; Elsevier: Amsterdam, 2001.
- (26) Bakhmutov, V. I. *Dihydrogen Bonds: Principles, Experiments, and Applications*; John Wiley & Sons: Hoboken, NJ, 2008.
- (27) Besora, M.; Lledos, A.; Maseras, F. *Chem. Soc. Rev.* **2009**, *38*, 957–966.
- (28) Grabowski, S. J.; Sokalski, W. A.; Leszczynski, J. *Chem. Phys.* **2007**, *337*, 68–76.
- (29) Jacobsen, H. *Chem. Phys.* **2008**, *345*, 95–102.

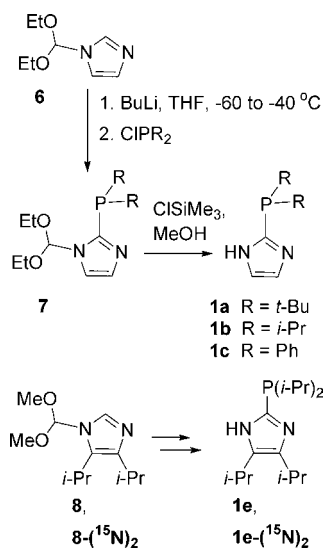
In the work reported here, three distinctly different hypotheses were advanced to explain changes in spectroscopic data. Below, after sections on study design, sample synthesis, and X-ray diffraction results, we describe the different hypotheses in turn and the evidence for and against the first two for one complex, which led us to develop the third. A series of spectral data were necessary, culminating in ¹⁵N chemical shifts obtained by observing natural abundance samples using ¹H–¹⁵N gradient HMBC and HSQC experiments, as well as data on selected compounds with ¹⁵N isotopic enrichment at both imidazole nitrogens. Calculations using density functional theory (DFT) were also needed to discriminate between two very different explanations of observed spectral changes. This work highlights the difficulties in studying fluxional or hemilabile organometallic systems containing bifunctional ligands.

Results and Discussion

Design of the Study. The rich and unusual chemistry enabled by the Cp*Ir fragment^{30–35} led us to explore it as a platform. In particular, chloro and hydride complexes of Cp*Ir monophosphine fragments have been versatile starting materials or intermediates. Therefore, using five ligands (**1a–1e**), we chose to make a concise series of complexes (Scheme 1) to explore the inter-relationship of phosphine R group (**a, b, c**) and hydride

- (30) Maitlis, P. M. *Coord. Chem. Rev.* **1982**, *43*, 377–384.
- (31) Bergman, R. G. *J. Organomet. Chem.* **1990**, *400*, 273–282.
- (32) Klei, S. R.; Golden, J. T.; Burger, P.; Bergman, R. G. *J. Mol. Catal. A* **2002**, *189*, 79–94.
- (33) Liu, J.; Wua, X.; Iggoa, J. A.; Xiao, J. *Coord. Chem. Rev.* **2008**, *252*, 782–809.
- (34) Fujita, K.-i.; Enoki, Y.; Yamaguchi, R. *Tetrahedron* **2008**, *64*, 1943–1954.
- (35) Moussa, J.; Amouri, H. *Angew. Chem., Int. Ed.* **2008**, *47*, 1372–1380.

Scheme 2. Ligand Synthesis



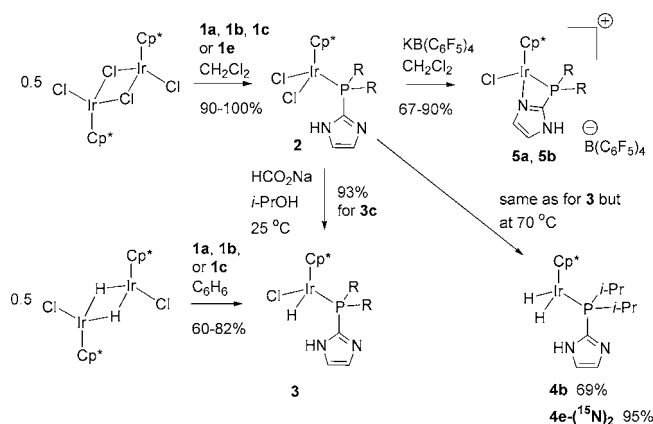
or chloride (**2**, **3**, **4**) on hydrogen bonding, using two nonheterocyclic complexes (**2d**, **3d**) incapable of hydrogen bonding as controls. In addition, later in the study, ligand **1e** was made to examine the role of *intermolecular* interactions of the imidazole, which would be reduced or eliminated by the presence of the isopropyl groups on the heterocycle. Finally, as discussed in more detail below, **1e-(^{15}N)₂** and its complexes were made to fully characterize *intramolecular* interactions of the imidazole nitrogens.

Synthesis. Ligand **1a** was made as we previously reported (Scheme 2),¹⁴ by lithiation of N-protected imidazole **6**,³⁶ addition of the requisite chlorophosphine, and subsequent deprotection by a trace of acid generated in situ by adding chlorotrimethylsilane to methanol. Ligand **1b** is new but made in a similar manner.³⁷ Ligand **1c** has been reported but without details of its synthesis or characterization data;^{38–40} the procedure reported here gives 69% yield. Our observations suggest that better yields result from using as little acid as possible and using methanol rather than water for the deprotection step.⁴¹ Ligand **1e** was made in a similar fashion from known precursor **8**,³⁶ as was its doubly labeled isotopomer **1e-(^{15}N)₂**.³⁷

All five ligands (**1a–1e**) and isotopomer **1e-(^{15}N)₂** were used to break dimer $[\text{Cp}^*\text{Ir}(\text{Cl})(\mu\text{-Cl})_2]$ (Scheme 3). As monitored by NMR spectroscopy, reactions of the less hindered ligands **1b**, **1c**, and **1d** were complete within minutes at ambient temperature, whereas that of the di-*tert*-butyl ligand **1a** was slower. Spectral and other data for the products will be discussed below.

The monohydride monochloride complexes **3** were made in a similar fashion by breaking dimer⁴² $[\text{Cp}^*\text{Ir}(\text{Cl})(\mu\text{-H})_2]$. Here,

Scheme 3. Syntheses of Imidazolylphosphine Complexes



however, reaction progress could be determined not only by ^1H and ^{31}P NMR spectroscopy but also visually: the starting dimer is an intensely blue solid, whereas the products are orange-yellow, albeit somewhat less intensely colored than the dichloride complexes. As in the dichloride case, the less hindered ligands **1b**, **1c**, and **1e-(^{15}N)₂** reacted more quickly (at room temperature within 1 day), whereas di-*tert*-butyl ligand **1a** required nearly a week of heating at 70 °C to complete its reaction. Intriguingly, model ligand **1d**, which should have the same steric profile as **1b** or **1c** and therefore react just as quickly, required days at 70 °C to completely break dimer $[\text{Cp}^*\text{Ir}(\text{Cl})(\mu\text{-H})_2]$, which may suggest a role for hydrogen bonding in breaking the hydride dimer when the imidazolylphosphines are used. In the case of **3c**, cleaner product was obtained by selectively reducing **2c** with sodium formate in methanol.

Dihydride complex **4b** was made by reducing **2b** with sodium formate (5 to 6 mol per mol of **4b**) in methanol. After 14 h at ambient temperature, analysis of the mixture by ^1H and ^{31}P NMR spectroscopy showed the complete consumption of **2b**, formation of mostly (>90%) monohydride **3b**, along with traces of **4b**. In contrast, when a similar mixture was heated at 70 °C for 24 h, reduction was complete, allowing isolation of **4b** as a nearly colorless solid in 69% yield. A solution of **4b** in oxygen-free, dry C_6D_6 was stable for more than a month at room temperature, and a solution in CD_2Cl_2 appeared to contain only traces (<2%) of **3b** after 2 days at room temperature. Model dihydride complex **4d** was made from **2d** by a similar procedure, though interestingly, reduction of **2d** seemed to require a greater excess of formate and longer reaction times.

The monohydride products **3** occasionally contained traces (<2%) of other hydride species, including the corresponding dihydride. In addition, some attempts at recrystallizing the monohydrides **3a** and **3b** led to isolation of a first crop of crystals of the corresponding dichlorides **2a** or **2b**, even when all chlorinated solvents were avoided. Presumably, this means that there was a conproportionation of two molecules of **3** to give one molecule each of **2** and **4**, but only **2** was isolated. Interestingly, solutions of **3a** and **3b** in oxygen-free, dry C_6D_6 were stable for weeks at room temperature, suggesting that the putative conproportionation may be driven by crystallization of the least-soluble compound **2** under certain conditions.

To explore the effect of ionizing the chloride ligand, **2a** and **2b** were treated with $\text{KB}(\text{C}_6\text{F}_5)_4$ to give **5a** and **5b**, respectively, in 67–90% isolated yield.

X-ray Structures. X-ray quality crystals of four dichloride complexes (**2a**, **2b**, **2c**, **2e**), two monohydrides [**3b** and

(36) Curtis, N. J.; Brown, R. S. *J. Org. Chem.* **1980**, *45*, 4038–4040.

(37) For details of compound preparation and characterization, see Supporting Information.

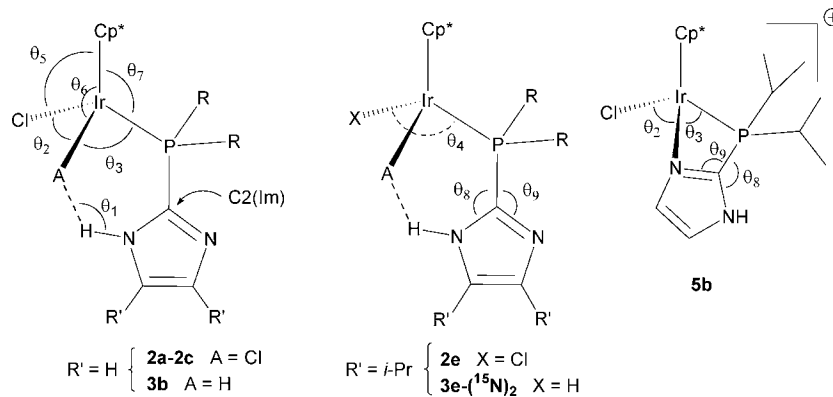
(38) Saxon, E.; Armstrong, J. I.; Bertozzi, C. R. *Org. Lett.* **2000**, *2*, 2141–2143.

(39) Spencer, L. P.; Altwer, R.; Wei, P.; Gelmini, L.; Gauld, J.; Stephan, D. W. *Organometallics* **2003**, *22*, 3841–3854.

(40) Chan, K. T. K.; Spencer, L. P.; Masuda, J. D.; McCahill, J. S. J.; Wei, P.; Stephan, D. W. *Organometallics* **2004**, *23*, 381–390.

(41) For synthesis of an analogue of **1** with methyl groups on phosphorus, see: Chen, Z.; Schmalke, H. W.; Fox, T.; Blacque, O.; Berke, H. J. *Organomet. Chem.* **2007**, *692*, 4875–4885.

(42) Gill, D. S.; Maitlis, P. M. *J. Organomet. Chem.* **1975**, *87*, 359–364.

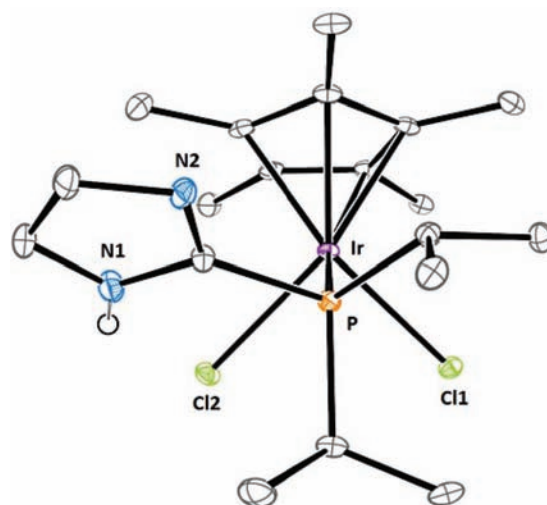
Table 1. Selected Bond Distances (Å) and Angles (deg)^a


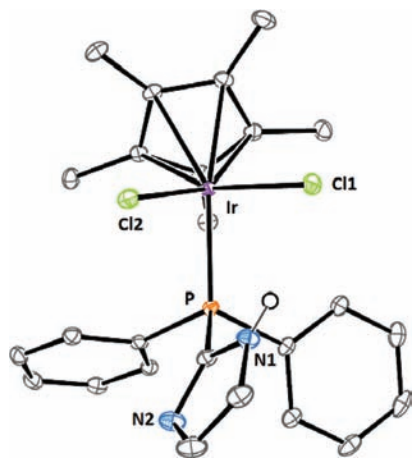
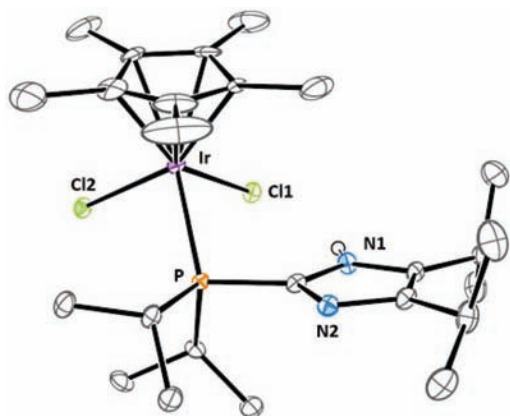
| | 2a | 2b | 2c | 2e | 3b | 3e-(¹⁵ N) ₂ | 5b |
|--|---------------|-------------|---------------|--------------|----------------|------------------------------------|-----------------|
| Ir–Cp* (Cp* = centroid) | 1.844(2) | 1.818(2) | 1.827(8) | 1.819(12) | 1.869(2) | 1.866(2) | 1.800(2) |
| Ir–P | 2.3957(6) | 2.3140(7) | 2.2972(7) | 2.3171(13) | 2.2645(11) | 2.2788(10) | 2.3841(8) |
| Ir–A (hydrogen bonded) (Ir–N for 5b) | 2.4224(5) | 2.4336(7) | 2.4263(7) | 2.4419(14) | 1.64(2) (Ir–H) | 2.4072(11) | 2.118(3) (Ir–N) |
| Ir–Cl or Ir–X (non-hydrogen-bonded) | 2.4005(5) | 2.4032(6) | 2.4089(7) | 2.4050(14) | 2.4097(13) | 1.664(19) | 2.4001(9) |
| P–C2(Im) | 1.835(2) | 1.807(3) | 1.820(3) | 1.804(5) | 1.821(3) | 1.820(4) | 1.799(3) |
| N–A | 3.054(4) | 3.177(8) | 3.202(3) | 3.141(4) | 2.55(2) | 3.039(4) | – |
| N–H | 0.88 | 0.88 | 0.79(3) | 0.87(7) | 0.900(1) | 0.88 | 0.87 |
| H···A | 2.27(1) | 2.44(1) | 2.47(3) | 2.40(7) | 1.913 | 2.29(2) | – |
| A to imidazole plane ^b | 0.337 | 0.588 | 0.115 | 0.651 | 0.220 | 0.863 | – |
| Cl or X to imidazole plane ^b | 2.593 | 0.797 | 2.741 | 0.723 | 2.538 | 1.722 | – |
| torsional angle C2(Im) P–Ir–Cp* | –175.65(0.36) | 62.58(0.35) | –165.96(0.34) | –66.34(0.52) | 163.58(0.53) | –179.59(0.37) | –134.55(0.34) |
| (θ ₁) N–H···A | 149.1(1) | 141.1(1) | 155(3) | 143(6) | 126.4 | 143.3(2) | – |
| (θ ₂) Cl–Ir–A, X–Ir–A, or Cl–Ir–N | 85.898(19) | 89.39(2) | 88.74(2) | 88.05(5) | 84.8(1) | 92.0(17) | 83.58(8) |
| (θ ₃) A–Ir–P or N–Ir–P | 91.932(18) | 86.39(2) | 91.33(2) | 87.10(5) | 79.7(3) | 95.31(4) | 66.88(7) |
| (θ ₄) Cl–Ir–P or X–Ir–P | 88.090(19) | 88.84(2) | 86.84(2) | 91.78(5) | 90.5(4) | 83.1(17) | 87.64(3) |
| (θ ₅) Cp*–Ir–Cl or Cp*–Ir–X | 120.6(1) | 123.5(1) | 122.4(3) | 122.1(4) | 122.4(1) | 121.19(4) | 122.6(1) |
| (θ ₆) Cp*–Ir–A | 117.5(1) | 122.2(1) | 123.6(3) | 124.0(4) | 125(3) | 117.55(2) | – |
| (θ ₇) Cp*–Ir–P | 138.5(1) | 133.5(1) | 131.4(2) | 131.1(4) | 137.3(1) | 136.03(3) | 140.6(1) |
| (θ ₈) P–C2(Im)–N(H) | 124.29(16) | 121.9(2) | 121.9(2) | 121.8(4) | 124.6(6) | 123.3(3) | 145.2(3) |
| (θ ₉) P–C2(Im)–N | 125.20(16) | 127.0(2) | 125.8(2) | 127.5(4) | 124.7(6) | 125.8(3) | 105.2(2) |

^a Cp* = centroid. ^b Distance to mean plane defined by the three carbons and two nitrogens of the imidazole ring.

3e-(¹⁵N)₂], and ionized chelate complex **5b were all obtained. Collection information is given in Table S1 in Supporting Information, whereas key bond length and angle data are in Table 1. Molecular structures are shown in Figures 1–7 and in Supporting Information Figure S1. In the case of **3b**, the positions of the NH and hydride hydrogens potentially involved in hydrogen bonding were refined, whereas those of all other hydrogens were refined as a riding model. For **3e-(¹⁵N)₂**, the hydrogen atom bound to the Ir was located on the difference map, its bond length refined to an acceptable range, and its position refined. All other hydrogen atoms were placed using a riding model. All structures show the complexes as essentially octahedral complexes, with distortions detailed below.**

Interestingly, all four dichloride structures (Figures 1–3 and Figure S1) show interaction of the NH with one of the two chloride ligands and lengthening of the Ir–Cl bond involved in the hydrogen bonding by 0.0174(14) to 0.0369(28) Å. This difference varies, as does the orientation of the NH with respect to the Ir–Cl unit. For the four dichloride complexes, the

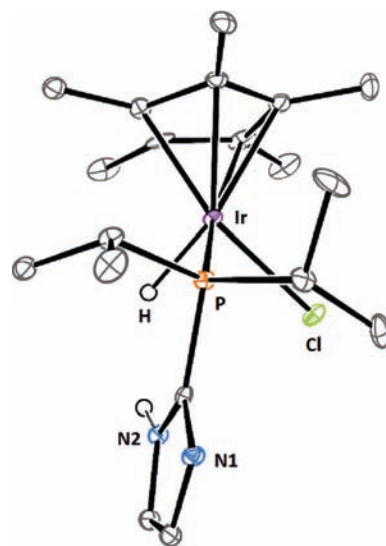
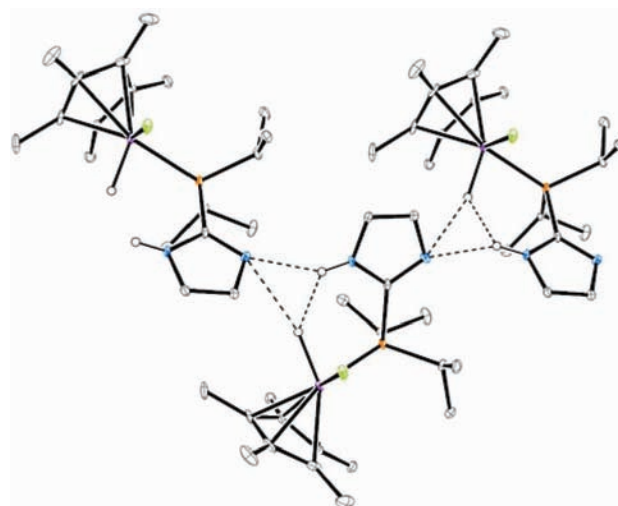
**Figure 1.** ORTEP structure of **2b**.

Figure 2. ORTEP structure of **2c**.Figure 3. ORTEP structure of **2e**.

N–H \cdots Cl angles are in the range of 141 to 155°, which is reasonably favorable for formation of a hydrogen bond.⁴³

Inspection of the angles formed between Cp* centroid and the three ligands (two chlorides and one phosphine) shows that the angles involving the phosphine (θ_7 , Table 1) are always significantly larger, by about 18–21° (**2a**), 10–11° (**2b**), 8–9° (**2c**), and 7–9° (**2e**), perhaps a reflection of the size of the two R groups on P. For each complex, the Cp*–Ir–Cl angle involving the chloride which is the hydrogen bond acceptor (θ_6) was smaller than the angle to the nonbonded chloride (θ_5), by about 1 to 3°.

In monohydride complex **3b** (Figure 4), the NH points toward the hydride ligand. As mentioned above, the position of the hydride was determined from the data, which show that the hydride nucleus is only 0.22 Å from the plane defined by the five atoms of the imidazole ring. This stands in contrast to the four structures of the dichloride complexes **2a–2c** and **2e**, where with the exception of **2c** the chloride accepting the NH hydrogen bond is further (0.34–0.67 Å) away from the imidazole ring plane. Additional distortions consistent with favorable hydrogen bonding are shown by comparing the P–Ir–Cl_A angle (θ_3) in **2b** and the analogous P–Ir–H_A angle in **3b**, where the latter is 6.7° less. The fact that in **3b** the NH points toward the hydride rather than the chloride and that the hydride–imidazole plane distance is smaller than analogous

Figure 4. ORTEP structure of the hydride complex **3b**.Figure 5. Intermolecular hydrogen bonding by complex **3b**.

distances involving chloride in **2a–2c** both suggested initially that the NH \cdots H–Ir dihydrogen bonding interaction is stronger than the one involving a chloride ligand, or that dihydrogen bonding is preferred for steric reasons because the hydride is smaller.⁴⁴ Below, we give spectroscopic and computational evidence contradicting this observation, which suggested in turn that the solution-state structure is different than that in the solid state. Indeed, inspection of the unit cell for **3b** (a part of which is shown in Figure 5) shows that the NH of one molecule points not only toward the hydride of the same molecule but also toward the basic imidazole nitrogen of an adjacent molecule. This intermolecular interaction appears to be unique among the complexes of this study.

To help determine whether intermolecular interactions in the solid state help favor dihydrogen bonding, analogue **3e** [made for other purposes as its (¹⁵N₂) isotopomer] with added steric hindrance from two isopropyl groups was analyzed by X-ray diffraction. Significantly, Figure 6 shows distinct preference for hydrogen bonding to chloride.

(43) Jeffery, G. A. *An Introduction to Hydrogen Bonding*; Oxford: New York, 1997.

(44) We thank a reviewer for suggesting that we consider the possibility that hydrogen bonding to hydride in **3b** might simply be a function of smaller size of the hydride ligand.

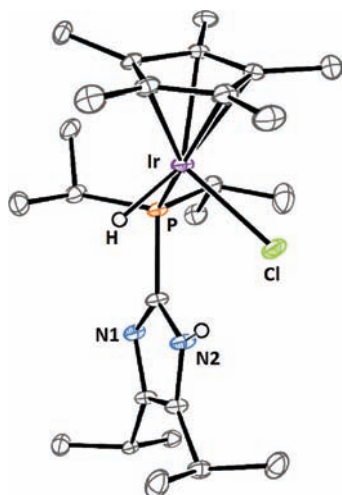


Figure 6. ORTEP structure of the hydride complex **3e**-¹⁵N₂.

In the absence of samples suitable for X-ray diffraction, NMR relaxation methods are often used to examine dihydrogen bonding to hydride ligands; fortunately, because the hydride position was located in the structure of **3b**, we have a more direct determination of the H⋯H distance (1.91 Å). This value is in line with distances seen in a variety of inter- and intramolecular dihydrogen bonds.^{15,21,22,45–47}

The solid-state structures of the dichloride complexes and **3b** and **3e**-¹⁵N₂ show two basic conformational preferences. If one considers the torsional angle defined by the Cp* centroid, Ir, P, and imidazolyl C2 atoms, then the conformations seen in the solid state can be called *anti* if the angle is near ±180° or *gauche* if near ±60°. Following this scheme, **2a**, **2c**, **3b** and **3e**-¹⁵N₂ would be *anti* and **2b** and **2e** *gauche*. Below, we show calculated structures of the two conformers that match the solid-state structures very well and low-temperature NMR data that also are completely consistent with the presence of *gauche* and *anti* conformers in solution.

Finally, the structure of **5b** (Figure 7) verifies that the imidazolylphosphine ligand is chelating and also verifies the distortions one would expect from a four-membered ring, such as a small (ca. 70°) P–Ir–N angle and therefore other larger intraligand angles.^{14,48,49}

NMR Spectroscopy and Three Hypotheses To Explain the Data. A combination of IR and NMR spectroscopic data, the latter at ambient and low temperatures, shows the effects of hydrogen bonding. In the course of this study, three distinctly different hypotheses (A, B, and C below) were advanced to account for the data obtained. Ultimately, complex **2a** was shown to differ significantly even from its homologue **2b**, revealing intriguing and unexpected differences caused by the size of R groups on phosphorus. Experiments and calculations allowed us to reject hypothesis A and conclude that hypothesis

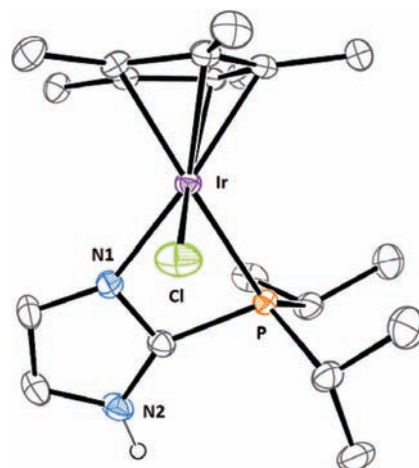


Figure 7. ORTEP structure of the cation of **5b**.

B appears to apply to all complexes in this work and to **2a** under conditions (C₆D₆, toluene-*d*₈, THF-*d*₆) where ionization is disfavored. In even slightly more polar or hydrogen bonding solvents, **2a** undergoes ionization (hypothesis C) to varying degrees.

Table 2 shows selected ¹H and ³¹P NMR data for the complexes in this study. Similar data for the ligands and full tables of ¹³C NMR data appear in Supporting Information, along with details of their assignments using a combination of ¹H, ¹³C{¹H}, COSY, HSQC, and HMBC data. In addition, in selected cases, ROESY (**4b**) and ¹H{³¹P} NMR data were obtained in order to differentiate the two imidazolyl CH protons and the isopropyl methyl protons and to resolve the small couplings shown by the imidazole CH proton peaks. The assignments for the imidazolyl protons and carbons match those found for simple imidazole derivatives.^{50,51}

From inspection of the NMR data, several trends emerge. All of the *hydride* complexes of imidazolylphosphines (**3a**, **3b**, **3c**, **4b**) appeared as single species in *all solvents examined* (C₆D₆, toluene-*d*₈, CDCl₃, and CD₂Cl₂), and *at all temperatures examined*. For dichloride complex **2c**, the same observation was made, whereas for **2b** or **2e**, signals for two species could be seen at low temperatures in either toluene-*d*₈ or CD₂Cl₂. In contrast, solutions of **2a** in toluene-*d*₈ or C₆D₆ revealed the presence of a single species at all temperatures examined, but solutions in CDCl₃ and CD₂Cl₂ showed two sets of NMR resonances, even at ambient temperatures.

Our initial hypothesis (A in Scheme 4) was that, for both **2a** and **2b**, the two species differ in orientation of the imidazole ring, where in conformer **2-endo** the imidazole NH is pointed toward one chloride ligand, as shown in the solid-state structures, and in **2-exo** the imidazole ring would be turned 180°, with the NH pointing away from the chlorides. The ratios of these two proposed species could have been taken as indications of relative hydrogen bonding strength. However, we note that the conformers shown in hypothesis B are precisely what are seen in the solid-state structures of **2a** and **2c** (*endo-anti*) and **2b** and **2e** (*endo-gauche*). Furthermore, calculations (see below) also ultimately lead to rejection of hypothesis A because the *exo* conformers were predicted to be 5.8 to 12.5 kcal mol⁻¹ less stable, depending on

(45) Jessop, P. G.; Morris, R. H. *Coord. Chem. Rev.* **1992**, *121*, 155–284.

(46) Shubina, E. S.; Belkova, N. V.; Krylov, A. N.; Vorontsov, E. V.; Epstein, L. M.; Gusev, D. G.; Niedermann, M.; Berke, H. *J. Am. Chem. Soc.* **1996**, *118*, 1105–1112.

(47) Bakhmutov, V. I.; Bakhmutova, E. V.; Belkova, N. V.; Bianchini, C.; Epstein, L. M.; Masi, D.; Peruzzini, M.; Shubina, E. S.; Vorontsov, E. V.; Zanobini, F. *Can. J. Chem.* **2001**, *79*, 479–489.

(48) Grotjahn, D. B.; Gong, Y.; Zakharov, L. N.; Golen, J. A.; Rheingold, A. L. *J. Am. Chem. Soc.* **2006**, *128*, 438–453.

(49) Miranda-Soto, V.; Perez-Torrente, J. J.; Oro, L. A.; Lahoz, F. J.; Martin, M. L.; Parra-Hake, M.; Grotjahn, D. B. *Organometallics* **2006**, *25*, 4374–4390.

(50) Padilla-Martinez, I. I.; Ariza-Castolo, A.; Contreras, R. *Magn. Reson. Chem.* **1993**, *2*, 189–193.

(51) Takeuchi, Y.; Yeh, H. J. C.; Kirk, K. L.; Cohen, L. A. *J. Org. Chem.* **1978**, *43*, 3565–3570.

Table 2. Proton and Phosphorus NMR Data for Complexes in This Study^a

| compound | solvent (temp) ^a | 1H | | | | | | 31P{1H} |
|----------|--|---|-----------------------------|---|----------------------------|---|--------------------------------|---------|
| | | C5(CH3)5 | Ir-H | NH | ImCH or iPr | ImCH or iPr | R ₂ P | |
| 2a | C ₆ D ₆ CD ₂ Cl ₂ | 1.20 (d, J = 1.0, 15H) | 12.51 (br s, 1H) | 7.22 (s, 1H) | 6.53 (s, 1H) | 1.44 (d, J = 14.5, 18H) | 27.2 (sl br s) | |
| | | 2a: ^b 1.57 (d, J = 1.0, 15H) | 2a: 12.19 (br s, 1H) | 2a: 7.13 (s, 1H) | 2a: 7.06 (s, 1H) | 2a: 1.40 (d, J = 14.5, 18H) | 2a: 27.4 (sl br s) | |
| | | 5a-Cl: ^c 1.76 (d, J = 2.5, 15H) | 5a-Cl: 16.0 (very br s, 1H) | 5a-Cl: 7.09 (s, 1H) | 5a-Cl: 7.00 (br s, 1H) | 5a-Cl: 1.64 (sl br d, J ≈ 16, 9H), ~1.39 (broad peak obscured, 9H) | 5a-Cl: ca. 27 (very br) | |
| 2c | CD ₂ Cl ₂ (-60°C) | 2a: ^c 1.51 (d, J = 2.5, 15H) | 2a: 12.26 (br s, 1H) | c | | 2a: 1.31 (d, J = 14.5, 18H) | 2a: 26.8 (s) | |
| | | 5a-Cl: ^c 1.70 (d, J = 1.5, 15H) (ratio 1 to 1) | 5a-Cl: 15.6 (very br s, 1H) | | | 5a-Cl: 0.59 (br d, J ≈ 15, 3H), 1.49 (partially obscured d, 3H), 1.55 (d, J = 16.0, 9H), 1.74 (br d, J ≈ 12, 3H) | 5a-Cl: 25.8 (very br) | |
| | | 2a: ^d 1.57 (d, J = 1.6, 15H) | 2a: 12.17 (br s, 1H) | 2a: 7.05 (s, 1H) | 2a: 7.02 (br s, 1H) | 2a: 1.40 (d, J = 14.4, 18H) | 2a: 27.4 (sl br s) | |
| 2b | C ₆ D ₆ | 5a-Cl: ^d 1.76 (d, J = 2.4, 15H) | 5a-Cl: 15.93 (br s, 1H) | 5a-Cl: 7.16 (s, 1H) | 5a-Cl: 7.02 (br s, 1H) | 5a-Cl: 1.64 (d, J = 16.8, 9H), ~1.39 (broad peak obscured, 9H) | 5a-Cl: ca. 27 (very br) | |
| | | 1.17 (d, J = 1.8, 15H) | 11.79 (br s, 1H) | 7.14 (s, 1H) | 6.46 (s, 1H) | 3.13 (br featureless peak, w _{1/2} = 30 Hz, 2H), 1.47 (dd, J = 7.2, 15.7, 6H), 1.24 (sl br dd, J ≈ 7, 15, 6H) | -0.1 (sl br s) | |
| | | 1.52 (d, J = 2.0, 15H) | 11.55 (br s, 1H) | 7.14 (sl br s, 2H) | | 3.07 (septet of d, ³ J _{HH} = 7.3, ² J _{HP} = 9.5, 2H), 1.36 (dd, J = 7.2, 15.6, 6H), 1.27 (dd, J = 7.2, 15.2, 6H) | 1.7 (sl br s) | |
| 2d | CD ₂ Cl ₂ (-45°C) | anti: ^e 1.62 (s, 15H) | anti: 12.16 (sl br s, 1H) | anti: ^{e,f} 7.13 (sl br s, 2H) | | anti: ^{e,g} 2.80-2.92 (m, 2H) | anti: ^e 7.4 (sharp) | |
| | | gauche: 1.28 (s, 15H) | gauche: 11.00 (sl br s, 1H) | gauche: 7.19 (sl br s, 1H) | | | | |
| | | anti: ^h 1.61 (sl br s, 15H) | anti: 12.19 (1H) | anti: 7.14 (sl br s, 1H) | gauche: 7.05 (sl br s, 1H) | gauche: 3.42 and 2.80 (very br, 1H each) | gauche: -4.3 (sharp) | |
| 2c | CD ₂ Cl ₂ (-90°C) | gauche: 1.27 (sl br s, 15H) | gauche: 10.98 (1H) | gauche: 7.19 (sl br s, 1H) | anti: 7.12 (sl br s, 1H) | anti: 2.85-2.95 (m, 2H), 1.07 (dd, ³ J _{HH} = 7.0, ² J _{HP} = 16.8, 6H), 0.98 (dd, ³ J _{HH} = 6.7, ² J _{HP} = 14.4, 6H) | nd | |
| | | 1.39 (d, J = 2.5, 15H) | 11.24 (br s, 1H) | 7.10 (br s, 2H) | gauche: 7.04 (sl br s, 1H) | gauche: 3.36-3.47 and 2.76-2.85 (featureless m, 1H each), 1.73 (sl br dd, ³ J _{HH} ≈ 7, ² J _{HP} ≈ 13, 3H), 1.54 (sl br dd, ³ J _{HH} ≈ 7, ² J _{HP} ≈ 18, 3H), 1.39 (sl br dd, ³ J _{HH} ≈ 7, ² J _{HP} ≈ 18, 3H), 1.27 (s, 15H), 0.76 (sl br dd, ³ J _{HH} ≈ 7, ² J _{HP} ≈ 14, 3H) | gauche: -6.2 (sl br s) | |
| | | 1.41 (d, J = 2.2, 15H) | 11.6 (br s, 1H) | 7.13 (br s, 2H) | | 7, 11, 4H), 7.42-7.51 (m, 6H) | -5.1 (sl br s) | |
| 2d | CDCl ₃ | 1.28 (d, J = 2.0, 15H) | | For Ph: 7.71-7.75 (m, 2H), 7.38-7.42 (m, 2H), 7.32-7.36 (m, 1H) | | 1.22 (dd, J = 7.2, 13.2, 6H), 1.58 (dd, J = 7.2, 16.0, 6H), 3.17-3.31 (m, 2H) | 0.5 (s) | |

Table 2. Continued

| compound | solvent (temp) ^a | C ₅ (CH ₃) ₅ | Ir-H | NH | ImCH or iPr | ImCH or iPr | R ₂ P | ³¹ P{ ¹ H} |
|--|--|---|--|--|--|-------------|---|--|
| 2e | CDCl ₃ | 1.45 (d, <i>J</i> = 1.7, 15H) | 10.68 (br s, 1H) | 3.00 (septet, ³ J _{HH} = 7.0, 1H), 1.184 (d, ³ J _{HH} = 7.0, 6H) | 2.87 (septet, ³ J _{HH} = 7.0, 1H), 1.194 (d, ³ J _{HH} = 7.0, 6H) | | 3.06–3.22 (m, 2H), dd at about 1.45 (6H) overlapping with Cp* signal, 1.22–1.34 (m, 6H) | –4.1 (sl br s) |
| 2e-(¹⁵N)₂ | CD ₂ Cl ₂ | 1.46 (d, <i>J</i> = 1.98, 15H) | 10.81 (d, ¹ J _{HN} = 95.40, 1H) | 3.02 (d of septet, ³ J _{HN} = 2.98, ³ J _{HH} = 6.94, 1H), 1.212 (d, ³ J _{HH} = 6.95 or 6.74, 6H) | 2.90 (dd of septet, <i>J</i> = 0.60, ³ J _{HN} = 2.97, ³ J _{HH} = 6.88, 1H), 1.199 (d, ³ J _{HH} = 6.74 or 6.95, 6H) | | 3.02–3.16 (m, 2H), 1.42 (dd, ³ J _{HH} = 7.34, ² J _{HP} = 15.87, 6H), 1.28 (sl br dd, ² J _{HP} = 7.2, ² J _{HP} = 14.6, 6H) | –3.0 (sl br s) |
| 3a | C ₆ D ₆ | anti: 1.60 (s, 15H minor) 1.55 (d, <i>J</i> = 1.2, 15H) | anti: 11.87 (d, ¹ J _{HN} = 95.21, 1H) 11.40 (br s, 1H) | 7.30 (s, 1H) | 6.52 (s, 1H) | | gauche: 3.37 (sl br d of septet, ³ J _{HH} ≈ ² J _{HP} ≈ 8, 1H), 2.92–3.02 (m, 1H), 1.66 (sl br dd, ³ J _{HH} ≈ 6.7, ² J _{HP} ≈ 12.3, 3H), 1.52 (sl br dd, ³ J _{HH} ≈ 7.1, ² J _{HP} = 15.9, 3H), 1.36 (dd, ³ J _{HH} = 7.6, ² J _{HP} = 17.6, 3H), 0.78 (dd, ³ J _{HH} = 7.3, ² J _{HP} = 14.2, 3H) | gauche: –6.0 (t, ² J _{PN} = ² J _{PN'} = 10.0) |
| 3b | C ₆ D ₆ | 1.59 (dd, <i>J</i> = 0.9, 1.8, 15H) | 11.85 (br s, 1H) | 7.25 (sl br s, 1H; decoupling of ³¹ P led to dd, <i>J</i> = 1.0, 1.7) | 6.50 (~sl br dd, <i>J</i> ≈ 1.0, 2.4, 1H; decoupling of ³¹ P led to dd, <i>J</i> = 1.0, 2.2) | | 1.42 (d, ³ J _{HP} = 14.4, 9H), 1.35 (d, ³ J _{HP} = 14.4, 9H), 2.86 (septet of d, ³ J _{HH} = 7.0, ² J _{HP} = 9.7, 1H), 2.56 (septet of d, ³ J _{HH} = 7.0, ² J _{HP} = 8.8, 1H), 1.29 (³ J _{HH} = 7.0, ³ J _{HP} = 15.4, 3H), 1.211 (³ J _{HH} = 7.0, ³ J _{HP} = 16.1, 3H), 1.205 (³ J _{HH} = 7.0, ³ J _{HP} = 15.3, 3H), 0.96 (dd, ³ J _{HH} = 7.0, ³ J _{HP} = 16.4, 3H) | anti: +4.4 (t, ² J _{PN} = ² J _{PN'} = 9.9) |
| 3c | CD ₂ Cl ₂ | 1.81 (narrow m) | 11.34 (br s, 1H) | 7.16 (sl br s, 1H) | 7.08 (narrow m, 1H) | | 2.74 (septet of d, <i>J</i> = 7.1, 9.5), 2.61 (septet of d, <i>J</i> = 7.1, 8.9), 1.21 (dd, <i>J</i> = 7.1, 16.7) | –13.7 |
| 3d | C ₆ D ₆ CD ₂ Cl ₂ | not sol 1.59 (d, <i>J</i> = 2.0, 15H) | 11.42 (br s, 1H) | 7.17 (sl br s, 1H) | 7.09 (narrow m, 1H) | | 7.86–7.92 (m, 2H), 7.42–7.46 (m, 3H), 7.32–7.40 (m, 5H), 2.83 (septet of d, ³ J _{HH} = 7.2, ² J _{HP} = 11.2, 1H), 2.67 (septet of d, ³ J _{HH} = 7.2, ² J _{HP} = 8.4, 1H), 1.22 (dd, ³ J _{HH} = 7.2, ³ J _{HP} = 14.8, 3H), 1.13 (dd, ³ J _{HH} = 7.2, ³ J _{HP} = 15.0, 3H), 1.08 (dd, ³ J _{HH} = 7.2, ³ J _{HP} = 15.7, 3H), 0.89 (dd, ³ J _{HH} = 7.2, ³ J _{HP} = 13.8, 3H) | –3.3 28.9 |
| 3d | C ₆ D ₆ | 1.57 (dd, <i>J</i> = 1.0, 1.9, 15H) | –13.88 (d, 36.7) | For Ph: 7.52 (~t, <i>J</i> ≈ 8, 2H), 7.11 (~t, <i>J</i> ≈ 8, 2H), 7.02–7.08 (m, 1H) | | | | |

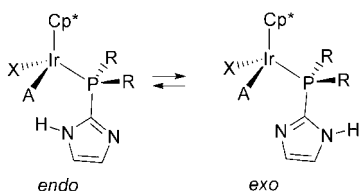
Table 2. Continued

| compound | solvent (temp) ^a | 1H | | | | | | 31P{1H} |
|--|--|--|---------------------------------|---|--|---|---|---------|
| | | C ₅ (CH ₆) ₅ | Ir-H | NH | ImCH or iPr | ImCH or iPr | R ₂ P | |
| 3e -(¹⁵ N) ₂ | C ₆ D ₆ | 1.59 (dd, <i>J</i> = 0.9, 1.5, 15H) | -14.01 (d, <i>J</i> = 38.7, 1H) | 11.66 (d, ¹ <i>J</i> _{NH} = 95.06, 1H), | 2.93 (d of septet ^g , <i>J</i> = 2.9, 7.0), 2.81 (d of septet, <i>J</i> = 2.9, 7.0, 1H), 1.461 and 1.451 (two overlapping d, <i>J</i> = 6.79, total 6H), 1.16 (d, <i>J</i> = 6.99, 3H), 1.09 (d, <i>J</i> = 6.99, 3H) | 2.87–2.95 (m) (overlapping with signal for ring <i>i</i> -Pr), 2.47–2.55 (m, 1H), 1.297 (dd, <i>J</i> = 6.99, 15.38, 3H), 1.243 (dd, <i>J</i> = 6.99, 19.97, 3H), 1.216 (dd, <i>J</i> = 6.99, 14.98, 3H), 0.99 (dd, <i>J</i> = 7.29, 16.08, 3H), 1.12 (dd, ³ <i>J</i> _{NH} = 7.0, ³ <i>J</i> _{HP} = 14.8, 6H), 0.96 (dd, ³ <i>J</i> _{NH} = 7.0, ³ <i>J</i> _{HP} = 16.8, 6H) | -10.6 (narrow m - maybe dt, <i>J</i> = 10.0, 12.0). | |
| 4b | C ₆ D ₆ | 2.07 (td, ¹ <i>J</i> _{NH} = 0.9, ³ <i>J</i> _{HP} = 1.8, 15H) | -18.27 (d, <i>J</i> = 30.6, 2H) | 10.03 (br s, 1H) | 7.41 (narrow m, 1H) | 6.36 (td, <i>J</i> = 1.5, 1.8, 1H) | 24.9 | |
| | CD ₂ Cl ₂ | 2.14 (s, 15H) | -18.70 (d, <i>J</i> = 30.2, 2H) | 10.20 (br s, 1H) | 7.28 (sl br s, 1H) | 7.02 (sl br s, 1H) | 25.5 | |
| 4d | C ₆ D ₆ | 2.05 (s, 15H) | -18.25 (d, <i>J</i> = 31.7, 2H) | | For Ph: 7.66 (~t, <i>J</i> ≈ 8, 2H), 7.19 (~t, <i>J</i> ≈ 8, 2H), 7.11 (~t, <i>J</i> ≈ 8, 1H) | 1.97–2.06 (m, 2H), 1.00 (dd, ³ <i>J</i> _{NH} = 6.5, ³ <i>J</i> _{HP} = 15.1, 6H), 0.80 (dd, ³ <i>J</i> _{NH} = 7.2, ³ <i>J</i> _{HP} = 14.4, 6H) | 41.6 | |
| 4e -(¹⁵ N) ₂ | C ₆ D ₆ | 2.08 (sl br s, 15H) | -18.20 (d, <i>J</i> = 39.9, 2H) | 9.85 (d, ¹ <i>J</i> _{NH} = 95.32) | 2.88 (d of septet, <i>J</i> = 2.8, 6.9, 1H), 2.70 (d of septet, <i>J</i> = 2.9, 6.9, 1H), 1.43 (dd, <i>J</i> = 0.64, 6.89, 6H), 0.95 (dd, <i>J</i> = 0.64, 7.05, 6H), | 2.48 (d of septet with ³ <i>J</i> _{NH} ≈ ³ <i>J</i> _{HP} = 7.0, 2H), 1.14 (dd, <i>J</i> = 6.89, 14.74, 6H), 1.01 (dd, <i>J</i> = 7.05, 16.66, 6H) | 23.4 (dd, <i>J</i> _{NH} = 9.5, 11.0) | |
| 5a | acetone- <i>d</i> ₆ | 1.85 (d, <i>J</i> = 2.5, 15H) | | not detectable | 7.57 (t, <i>J</i> = 1.2, 1H) | 7.37 (d, <i>J</i> = 1.3, 1H) | 28.1 (s) | |
| 5b | C ₆ D ₆ CD ₂ Cl ₂ | Not sol 1.86 (sl br s, 15H) | | 10.68 (br s, 1H) | 7.28 (sl br s, 1H) | 7.02 (sl br s, 1H) | 7.0 (s) | |
| | acetone- <i>d</i> ₆ ⁱ | 1.93 (d, <i>J</i> = 2.4, 15H) | | 13.23 (br s, 1H) | 7.70 (sl br s, 1H) | 7.50 (sl br s, 1H) | 4.4 (s) ^j | |

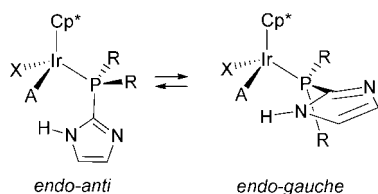
^a Chemical shifts in ppm, coupling constants in Hz. Measured at 30 °C unless otherwise specified. ^b Ratio of **2a** to **5-Cl** = 2:1. ^c Ratio of **2a** to **5-Cl** = 1:1. Also at -20 °C, ratio was 1:1. Because of this, it was not possible to assign which imidazole CH proton was associated with which species: slightly broadened singlets were seen at 7.10, 7.09, 7.06, along with a broader one at 6.95 ppm. ^d Ratio of **2a** to **5-Cl** = 1:1.2. ^e Ratio of major to minor species 1.6:1, assigned as **2b-endo-gauche** and **2b-endo-anti**, respectively. ^f Assignments tentative. ^g Impossible to identify other resonances. ^h Ratio of major to minor species 1.4:1, assigned as **2b-endo-anti** and **2b-endo-gauche**, respectively. ⁱ Ratio of major to minor species 2:1:1, assigned as **2e-(¹⁵N)₂-endo-gauche** and **2e-(¹⁵N)₂-endo-anti**, respectively. Several peaks for minor species not clearly identifiable because of overlap. See Figure S2 in Supporting Information. ^j Proton data on sample at -40 °C, ³¹P data obtained at 30 °C.

Scheme 4. Three Hypotheses To Explain Observation of Two Species in Solution

Hypothesis A:
two rotamers about the P-imidazole bond

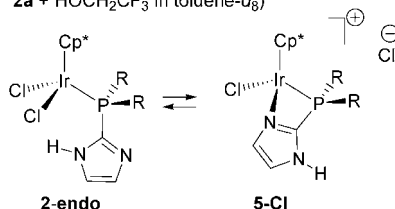


Hypothesis B:
two rotamers about the Ir-P bond



Hypothesis C: ionization

(applies to **2a** in CDCl₃, CD₂Cl₂, or more polar solvents, including **2a** + HOCH₂CF₃ in toluene-*d*₈)



whether a hydride or chloride was available for hydrogen bonding. All available NMR evidence is in accord with hypothesis C for **2a** in chlorinated or more polar solvents and hypothesis B for **2b** and all other cases in this study, as described next.

NMR Evidence Allowing Identification of Endo-anti and Endo-gauche Conformers. The ³¹P{¹H} NMR spectrum of **2b** in CD₂Cl₂ at -60 °C shows two sharp singlets at 7.3 (major) and -4.3 ppm (minor), with a ratio of 1.4:1, corresponding to a free energy difference of only 0.14 kcal mol⁻¹. Warming the latter solution to near 0 °C led to coalescence of the two peaks, which at 30 °C appeared as one slightly broad singlet at 1.7 ppm. Similar features were seen in proton NMR spectra of **2b**, with NH chemical shifts of 11.00 and 12.16, as well as ³¹P and ¹H spectra of analogous complex **2e**.

Though still slightly broadened at -90 °C, the ¹H resonances for the isopropyl groups on phosphorus in **2b** give a striking indication of the symmetry of each species: for the minor conformer, two broadened one-proton peaks ascribed to inequivalent methine protons were seen, whereas for the major conformer, only a single two-proton peak was observed. Moreover, for the minor species, *four* three-proton doublets of doublets between 0.76 and 1.73 ppm were visible, whereas for the major component, only *two* closely spaced six-proton doublets of doublets at 0.98 and 1.07 ppm were found. This would be consistent with the minor conformer being **2b-endo-gauche**, in which each methine is diastereotopic and also all four isopropyl methyls would be inequivalent. In contrast, although **2b-endo-anti** is chiral, it puts the isopropyl groups in a much more symmetrical environment; moreover, interconversion of the two enantiomers of **2b-endo-anti** involves only

a shift of the NH from one chloride ligand to the other one nearby and is predicted to have such a low barrier (1.4 kcal mol⁻¹) that the isopropyl groups of **2b-endo-anti** would be effectively equivalent. Very similar spectral changes were seen for more substituted complex **2e**, though here the **endo-gauche** conformer was slightly favored over the **endo-anti** one. The reversal of preference is not dramatic, however, involving a change of no more than about 1 kcal mol⁻¹. In principle, similar changes could be expected for spectra of **2c** because the phenyl rings in **2c-endo-gauche** would be diastereotopic, but either there is a stronger preference for one of the two conformers in this case or the activation energy for *gauche-anti* conversion is low enough that even at -90 °C sharp peaks could still be seen. Calculations (see below) predict that the barrier between *gauche* and *anti* conformers is 2.3–3.5 kcal mol⁻¹ lower for **2c** than for **2b** and **2e**, which could preclude detection of discrete conformers for **2c**.

Using line-shape analyses on ³¹P{¹H} NMR spectra, the activation parameters for interconversion of two conformers of **2b** in CD₂Cl₂ were measured as Δ*H*[‡] = 15.3 kcal mol⁻¹ and Δ*S*[‡] = +16 cal mol⁻¹ K⁻¹. It should be noted that the value of Δ*H*[‡] cannot be assigned only to breaking of whatever hydrogen bond might be present but also to changes in steric interactions during rotation around the bond between phosphorus and iridium C2. The strength of hydrogen bonding might be expected to be different in benzene or toluene than in either CDCl₃ or CD₂Cl₂ [*E*_T(30) values: CHCl₃, 39.1; CH₂Cl₂, 40.7; benzene, 34.3; toluene, 33.9].⁵² To test this hypothesis, VT NMR data for **2b** in toluene-*d*₈ were obtained, again showing two species equilibrating, but with Δ*H*[‡] = 9.4 kcal mol⁻¹ and Δ*S*[‡] = +3 cal mol⁻¹ K⁻¹, values lower than those seen in CD₂Cl₂, rather than higher as might be expected for breaking a stronger hydrogen bond.⁵³ Calculations (below) predict Δ*G*[‡] = 14.1 kcal mol⁻¹ for interconversion from *gauche* to *anti* in the gas phase, in reasonable agreement with our experimental results.

NMR Evidence for Ionization of 2a (Hypothesis C). Ionization of **2a** in CDCl₃ or CD₂Cl₂ to create a mixture of **5a-Cl** and **2a** seemed unlikely at first, given the fact that these solvents are not particularly polar. Nonetheless, numerous studies have shown the ability of chloroform or dichloromethane to donate hydrogen bonds,^{54–60} which (along with the NH of the cation of **5a-Cl**) could solvate chloride ion.

(52) Reichardt, C. *Solvents and Solvent Effects in Organic Chemistry*, 2nd ed.; VCH: New York, 1988.

(53) As for **2a**, it exhibited a single set of NMR peaks in C₆D₆, just like **2b**. However, unlike **2b**, for a sample of **2a** in toluene-*d*₈ (which is similar in solvent polarity to C₆D₆) between 30 and -60 °C, at all temperatures only a single set of resonances was seen, although the broadness of some resonances changed as a function of temperature. Some minor resonances were seen, but if these were indeed attributable to a second conformer, its amount would be at most 5%. Because for **2a** two species were easily detectable in either CDCl₃ or CD₂Cl₂ at 30 °C, it seemed much more probable that, in the aromatic solvents, a single species was seen rather than two very rapidly equilibrating ones. Observing a single species for **2a** in aromatic solvents is completely consistent with hypothesis C (see below) because it would be expected that ionization of chloride and formation of **5a-Cl** would be more favorable in chlorinated solvents because of their higher polarity and the possibility of hydrogen bonding of solvent to chloride ion.

(54) Gordy, W. *J. Chem. Phys.* **1939**, *7*, 167–171.

(55) Kamlet, M. J.; Taft, R. W. *J. Chem. Soc., Perkin Trans. 2* **1979**, 349–356.

(56) Kamlet, M. J.; Dickinson, C.; Taft, R. W. *J. Chem. Soc., Perkin Trans. 2* **1981**, 353–355.

(57) Oszczapowicz, J.; Thanh, B. P.; Oszczapowicz, I.; Wielogorska, E. *Mol. Phys. Rep.* **2001**, *33*, 87–89.

Table 3. ¹⁵N Chemical Shifts and Coupling Constants ¹J_{NH}^a

| compound(s) | solvent (temp) | species | N1 (NH or NCH ₃) | N3 (sp ² N) | δ _{N3} −δ _{N1} | ¹ J _{NH} (Hz) |
|---|--|----------------------------|--|---|----------------------------------|-----------------------------------|
| 1a | CD ₂ Cl ₂ | | −201.9 | not vis | nd | not vis |
| 1-methylimidazole | C ₆ D ₆ | | −223.5 | −115.7 | 107.8 | |
| | CDCl ₃ | | −220.5 | −122.8 | 99.7 | |
| | CD ₃ OD | | −216.0 | −133.1 | 82.9 | |
| | C ₆ D ₆ + CF ₃ CH ₂ OH | | −219.2 | −135.4 | 83.8 | |
| 1-methylimidazole + 2 CF ₃ CH ₂ OH | C ₆ D ₆ + CF ₃ CH ₂ OH | | | | | |
| 1e-(¹⁵N)₂ | C ₆ D ₆ | | −210.4 (d, <i>J</i> = 21.3) | −102.8 | 107.6 | 93.53 ^e |
| 2a | C ₆ D ₆ | | −193.3 | −99.4 | 93.9 | not vis |
| | CDCl ₃ | 2a | −194.4 ^b (2a) | −102.1 (2a) | 92.3 | not vis |
| | | 5a-Cl | −186.7 ^{b,c} (5a-Cl) | −203.9 (5a-Cl) | −17.2 | |
| | CD ₂ Cl ₂ | | −194.6 ^b (2a) | −100.7 (2a) | 93.9 | |
| | | | −185.5 (5a-Cl) | −203.3 (5a-Cl) | −17.8 | |
| 2b | C ₆ D ₆ | | −202.1 | −103.1 | 99.0 | not vis |
| | CDCl ₃ | | −202.8 | −107.4 | 95.4 | not vis |
| 2e | CDCl ₃ | | nd | nd | nd | 95.07 ^d |
| 2e-(¹⁵N)₂ | toluene- <i>d</i> ₈ | | −205.9 (d, ² J _{NP} = 8.4) | −104.9 (d, ² J _{NP} = 10.2) | 101.0 | 95.57 ^e |
| | toluene- <i>d</i> ₈ | endo-anti (minor) | −196.7 (d, ² J _{NP} = 9.7) | −103.4 (d, ² J _{NP} = 10.2) | 93.3 | 95.91 ^d |
| | (−80 °C) | endo-gauche (major) | −212.2 (d, ² J _{NP} = 9.3) | −108.7 (d, ² J _{NP} = 10.2) | 103.5 | 94.97 ^d |
| | CD ₂ Cl ₂ | | −208.3 (d, ² J _{NP} = 9.7) | −104.9 (sl br d, ² J _{NP} ≈ 11) | 103.4 | 95.40 ^e |
| | CD ₂ Cl ₂ (−80 °C) | endo-anti (minor) | −199.7 (d, ² J _{NP} = 9.3) | −103.7 (d, ² J _{NP} = 10.2) | 96.0 | 95.21 ^d |
| | | endo-gauche (major) | −213.6 (d, ² J _{NP} = 9.3) | −109.8 (d, ² J _{NP} = 10.2) | 103.8 | 95.45 ^d |
| 3a | C ₆ D ₆ | | −197.6 | −101.1 | 96.5 | 96.84 ^d |
| 3b | C ₆ D ₆ | | −201.0 | −102.8 | 98.2 | 96.92 ^d |
| 3e-(¹⁵N)₂ | toluene- <i>d</i> ₈ | | | | | |
| | toluene- <i>d</i> ₈ (−60 °C) | | −203.0 (d, <i>J</i> = 10.7) | −105.1 (d, <i>J</i> = 9.7) | 97.9 | 95.16 ^d |
| 4b | C ₆ D ₆ | | −201.6 | −106.4 | 95.2 | 97.12 ^d |
| 4e-(¹⁵N)₂ | C ₆ D ₆ | | −206.2 (dd, <i>J</i> = 1.0, 11.1) | −107.1 (d, <i>J</i> = 9.3) | 99.1 | 95.32 ^e |
| 5a | acetone- <i>d</i> ₆ | | −197.4 | −200.7 | −3.4 | not vis |
| 5b | acetone- <i>d</i> ₆ (−40 °C) ⁷² | | −197.0 ^b | −201.0 | −4.0 | not vis |

^a Samples at 30 °C unless otherwise specified. Unlabeled samples were examined using ¹H–¹⁵N gHMBC and in some cases gHSQC experiments. Parameters were chosen so as to give digital resolutions in the ¹⁵N dimension of 0.5 to 1.5 ppm. Labeled samples were examined using ¹⁵N{¹H} NMR experiments, typically with digital resolution of 0.8 Hz (0.015 ppm at 50.7 MHz). The ¹⁵N chemical shift of a standard reference sample of formamide solution in DMSO-*d*₆ (90%) was determined and set to be −267.8 ppm. Then, using the same sweep width and offsets, samples of nitromethane (1.0 M in CDCl₃) and quinine (0.5 M in CDCl₃) gave ¹⁵N chemical shifts of −4.2 for CH₃NO₂ and −72.4 and −349.2 ppm for the sp²- and sp³-hybridized nitrogens of quinine, respectively. ^b Identity verified by gHSQC experiment. ^c Identity verified by separate gHSQC experiment at −30 °C, where the low temperature was needed to allow the cross-peak to be seen. ^d Digital resolution 0.05 Hz. ^e Digital resolution 0.025 Hz.

To gain insight into the bonding environment of the second species formed from **2a**, an authentic sample of ionic complex **5a** was made from **2a** using KB(C₆F₅)₄, and data for it and **5b** were obtained, but ¹H and ³¹P NMR data did not allow conclusive identification of **5a-Cl**. However, one unusual ¹³C NMR resonance which strongly suggests formation of **5a-Cl** from **2a** in chlorinated solvents is the signal for C2 of the imidazole ring, whose chemical shift and small one-bond coupling constant [δ 153.4 ppm (d, ¹J_{CP} = 52.0 Hz)] match the data for chelate complexes **5a** and **5b** [**5a**: 155.1 (d, ¹J_{CP} = 44.3)] much better than data for **2a** [141.5 (d, ¹J_{CP} = 69.2)] and related **2b**, **2c**, and **2e**. We have previously observed downfield shift of C2 and diminution of ¹J_{CP} upon chelation by an imidazolylphosphine,^{14,48,61} along with other unusual NMR couplings which can be explained by altered bonding in the four-membered ring chelate. In striking contrast, the two species observed in low-temperature NMR spectra of **2b** show completely normal ¹J_{CP} for imidazole C2 (75 and 72 Hz), which would be consistent with relatively minor differences between *endo-anti* and *endo-gauche* conformers of **2b**.

¹⁵N NMR Data as Probe of Hydrogen or Metal Bonding to the Imidazolyl Group on the Phosphine. ¹⁵N chemical shifts can reveal a great deal about bonding at the nitrogen.^{62–67} Previous studies⁶⁷ of histidine and the model compound 1-methylimidazole showed the power of using ¹⁵N NMR data as a probe for hydrogen bonding or protonation of the imidazole nucleus. Thus, a series of ¹⁵N chemical shift data were obtained (Table 3) using natural abundance materials and ¹H–¹⁵N gHMBC and in some cases gHSQC experiments.^{68–70} These techniques worked well for imidazole derivatives without ring isopropyl groups because of strong cross-peaks between the ring protons and nitrogens; for **1e** and its complexes, the labeled derivative **1e-(¹⁵N)₂** and ¹⁵N direct detection were used instead.

- (58) Grushin, V. V.; Marshall, W. J. *Angew. Chem., Int. Ed.* **2002**, *41*, 4476–4479.
 (59) Chisholm, M. H.; Gallucci, J.; Hadad, C. M.; Huffman, J. C.; Wilson, P. J. *J. Am. Chem. Soc.* **2003**, *125*, 16040–16049.
 (60) Cerda, J. F.; Koder, R. L.; Lichtenstein, B. R.; Moser, C. M.; Miller, A.-F.; Dutton, P. L. *Org. Biomol. Chem.* **2008**, *6*, 2204–2212.
 (61) Grotjahn, D. B.; Zeng, X.; Cooksy, A. L.; Kassel, W. S.; DiPasquale, A. G.; Zakharov, L. N.; Rheingold, A. L. *Organometallics* **2007**, *26*, 3385–3402.

- (62) Schilf, W.; Stefaniak, L. In *New Advances in Analytical Chemistry*; Atta-ur-Rahman, Ed.; Harwood Academic: Amsterdam, 2000; p P1/659–P1/696.
 (63) Pazderski, L.; Szlyk, E.; Sitkowski, J.; Kamienski, B.; Kozerski, L.; Tousek, J.; Marek, R. *Magn. Reson. Chem.* **2006**, *44*, 163–170.
 (64) Marek, R.; Lycka, A.; Kolehmainen, E.; Sievanen, E.; Tousek, J. *Curr. Org. Chem.* **2007**, *11*, 1154–1205.
 (65) Marek, R.; Lycka, A. *Curr. Org. Chem.* **2002**, *6*, 35–66.
 (66) Andreeva, D. V.; Ip, B.; Gurinov, A. A.; Tolstoy, P. M.; Denisov, G. S.; Shenderovich, I. G.; Limbach, H.-H. *J. Phys. Chem. A* **2006**, *110*, 10872–10879.
 (67) Farr-Jones, S.; Wong, W. Y. L.; Gutheil, W. G.; Bachovchin, W. W. *J. Am. Chem. Soc.* **1993**, *115*, 6813–6819.
 (68) Foltz, C.; Enders, M.; Bellemin-Lapponnaz, S.; Wadepohl, H.; Gade, L. H. *Chem.—Eur. J.* **2007**, *13*, 5994–6008.
 (69) Baird, B.; Pawlikowski, A. V.; Su, J.; Wiench, J. W.; Pruski, M.; Sadow, A. D. *Inorg. Chem.* **2008**, *47*, 10208–10210.
 (70) Delp, S. A.; Munro-Leighton, C.; Khosla, C.; Templeton, J. L.; Alsop, N. M.; Gunnoe, T. B.; Cundari, T. R. *J. Organomet. Chem.* **2009**, *694*, 1549–1556.

In order to calibrate our data, we observed 1-methylimidazole (Table 3) in C_6D_6 , $CDCl_3$, and CD_3OD as did Farr-Jones et al.⁶⁷ and observed similar trends: the ^{15}N chemical shift of the basic nitrogen (N3) moved progressively upfield (by nearly 20 ppm) as the solvent's hydrogen bond donor ability increased, and the difference in nitrogen shifts $\delta_{N3}-\delta_{N1}$ decreased. Hydrogen bond donor CF_3CH_2OH added to a solution of 1-methylimidazole in C_6D_6 gave ^{15}N data resembling those in pure CD_3OD . Thus, if the basic imidazole nitrogen is involved in accepting a hydrogen bond from solvent (e.g., $CDCl_3$ or CD_2Cl_2), we should see upfield shifts for the N3 resonance or decrease in $\delta_{N3}-\delta_{N1}$. For **2b**, on going from C_6D_6 to $CDCl_3$, these values change only about half as much as for 1-methylimidazole N3 in the same two solvents.

Much more dramatic and diagnostic changes are seen in $CDCl_3$ when **2a** ($\delta_{N1} = -194.4$ and $\delta_{N3} = -102.1$ ppm), with shifts similar to those for **2b**, is partially converted to **5a-Cl**. The ionized species shows two ^{15}N peaks very close in chemical shift ($\delta_{N1} = -186.7$, but $\delta_{N3} = -203.9$ ppm), with the N1-H peak clearly assigned using gHSQC. The ^{15}N chemical shift data for preionized complexes **5a** and **5b** in acetone- d_6 match those for putative **5a-Cl** in $CDCl_3$ very well.

Careful observation of 1H NMR spectra for the NH peak of complex **3b** dissolved in C_6D_6 allowed determination of $^1J_{NH}$ (Table 3). A series of 1H decoupling experiments determined that narrow sharp triplets ($J = 1.8$ Hz) on either side of the broad major peak were the result of splitting by the imidazole ring protons, not the phosphorus. Integration of the minor peaks relative to the central broad peak was difficult due to overlap, but the integrals were consistent with the minor peaks being satellites from natural abundance ^{15}N at N1.⁷¹ The ^{15}N satellite peaks were only seen in spectra of hydride complexes **3a**, **3b**, or **4b**, whether in C_6D_6 or CD_2Cl_2 , but not for dichloride complexes **2a**, **2b**, or **2c**, even when samples of these species were cooled to -40 °C or lower to slow any possible NH exchange which might be masking $^1J_{NH}$.

Labeled compounds derived from **1e**-(^{15}N)₂ allowed determination of $^1J_{NH}$ under a wider variety of conditions, presumably because the ring isopropyl groups slowed NH exchange and also allowed observation at low temperatures of two distinct sets of ^{15}N peaks and $\delta_{N3}-\delta_{N1}$, which also appears to be sensitive to the nature of hydrogen bond donation by the imidazole NH. Absolute values of $^1J_{NH}$ increase from 93.53 Hz in free ligand **1e**-(^{15}N)₂ to 94.97–95.91 in the conformers of **2e**, to 95.16–95.32 in **3e** and **4e**. Shifting the NH interaction from chloride to hydride in **4e** weakens the interaction (because the chloride has a greater negative partial charge) but shortens the interaction distance (because hydride has a smaller ionic radius). Rather surprising is the sensitivity of $\delta_{N3}-\delta_{N1}$, where this value changes by nearly 10% between *endo-anti* and *endo-gauche* conformers of **2e**. This sensitivity to environmental change may be useful in other studies of bifunctional imidazole-based systems. Gratifyingly, the agreement between observed ^{15}N chemical shift changes in Table 3 and calculated values (Supporting Information, Table S33) is very good.

Influence of Solvent on Equilibrium between 2a and 5a-Cl and the Role of R on P in Promoting This Reaction. Having conclusively identified **5a-Cl**, the ratio of **2a** to **5a-Cl** as a function of solvent polarity and hydrogen bonding was exam-

ined. The least polar solvents [C_6D_6 , toluene- d_8 , and THF- d_8 ; $E_T(30)$ values⁵² 34.3, 33.9, 37.4] afforded **2a** exclusively. In contrast, $CDCl_3$ or CD_2Cl_2 gave mixtures with roughly similar amounts [$E_T(30)$ values: $CHCl_3$, 39.1; CH_2Cl_2 , 40.7]. The fact that $CHCl_3$ and THF are so similar by this measure but $CDCl_3$ gives so much more ionization suggests that chloride in **5a-Cl** may be solvated by hydrogen bonding to the C–D of $CDCl_3$. Acetone was a poor solvent, but CD_3NO_2 gave **2a** and **5a-Cl** in a 1:2 ratio, and what part of the sample did dissolve in *i*-PrOH- d_8 was more than 90% ionized (**5a-Cl**). Nitromethane and *i*-PrOH have $E_T(30)$ values of 46.3 and 48.4,⁵² respectively; the latter solvent could be expected to promote somewhat greater ionization by virtue of its polarity but in addition would be expected to solvate the chloride ion by hydrogen bonding to it.

Why would **2a** form ionized chelate **5a-Cl**, whereas **2b** would not form a similar species? Why would the un-ionized complex **2a** (whether observed alone or as a mixture with **5a-Cl** under conditions favoring ionization) appear to exist as a single conformer at all temperatures, whereas **2b** exists as a mixture of two conformers, **2b-endo-gauche** and **2b-endo-anti**? Both differences can be explained by the propensity of large substituents on acyclic systems to promote ring formation or cyclic intramolecular interactions. In organic chemistry, the Thorpe–Ingold effect and *gem*-dimethyl effect are classic expressions of this concept.^{73,74} In organometallic chemistry, it has been observed⁷⁵ that large substituents R on R_2PR^1 favor cyclometalation reactions at the third phosphine substituent R^1 , or that large ligand substituents can favor chelation.^{76–78} In this work, we find that hemilabile complexes show similar trends.

IR Spectroscopy. IR data (Table 4) were obtained in three ways, on freshly prepared C_6H_6 or CH_2Cl_2 solutions in CaF_2 cells or using reflectance on solid samples. The data for the three ligands in CH_2Cl_2 show the NH stretching frequency value in the absence of hydrogen bonding, which is approximately 3438 cm^{-1} . In chelate complexes **5a** and **5b**, which also would not have an intramolecular hydrogen bond, the NH absorption was slightly shifted but within 1% of the ligand value. Isotopic substitution by ^{15}N changes the position of absorption by about 0.2%.

In contrast, samples of the complexes **2b**, **2c**, **2e** and **3b**, **3c**, **3e** showed one or two bands for NH absorption, both in the range of $3189\text{--}3300\text{ cm}^{-1}$, and much broader than that seen for ligands **1a–1c**. In most cases when two bands were seen, one was a shoulder on the other, perhaps evidence of the two *endo-anti* and *endo-gauche* conformers. Calculated vibrational frequencies (Table S32) suggest that bands between 29 and 103 cm^{-1} apart might be seen for the two conformers, with the higher wavenumber value for the *anti* conformer. However, it appears that because *anti* and *gauche* conformers are so close in energy (e.g., from ratios seen for **2b** and **2e**-(^{15}N)₂ in CD_2Cl_2 at low temperature) variations in solvent and temperature could reverse which conformer is preferred.

The NH absorption for **4b** and **4e**-(^{15}N)₂ appeared outside the range seen for the complexes just discussed and closer to

(73) Jung, M. E.; Piizzi, G. *Chem. Rev.* **2005**, *105*, 1735–1766.

(74) Bachrach, S. M. *J. Org. Chem.* **2008**, *73*, 2466–2468.

(75) Shaw, B. L. *J. Organomet. Chem.* **1980**, *200*, 307–318.

(76) Sekabunga, E. J.; Smith, M. L.; Webb, T. R.; Hill, W. E. *Inorg. Chem.* **2002**, *41*, 1205–1214.

(77) Gallo, V.; Mastroianni, P.; Nobile, C. F.; Braunstein, P.; Englert, U. *Dalton Trans.* **2006**, 2342–2349.

(78) Arthur, K. L.; Wang, Q. L.; Bregel, D. M.; Smythe, N. A.; O'Neill, B. A.; Goldberg, K. I.; Moloy, K. G. *Organometallics* **2005**, *24*, 4624–4628.

(71) Katritzky, A. R.; Akhmedov, N. G.; Doskocz, J.; Mohapatra, P. P.; Hall, C. D.; Guven, A. *Magn. Reson. Chem.* **2007**, *45*, 532–543.

(72) Low temperature (-40 °C) was needed to resolve various ^{13}C resonances, as well.

Table 4. Infrared Data for Ligands and Complexes in This Study^a (Absorptions Listed Are for N–H Stretches unless Otherwise Specified)

| compound | sample medium | | |
|--|--|---|---|
| | C ₆ H ₆ | CH ₂ Cl ₂ | ATR |
| 1a | nd | 3438.3 (m) ^b | nd |
| 1b | nd | 3439.0 (m) ^c | nd |
| 1c | nd | 3438.1 (m) ^c | nd |
| 1e | nd | 3438.2 (m) | nd |
| 1e-(¹⁵N)₂ | nd | 3430.8 (m) | nd |
| 2a | 3305.3 (m) 3210.7 (m) | 3193.5 (m, br) ~3240 (sh) ~2400–2700 (m, very br) | 3225.4 (s, br) ~3300 (sh) 291.3, 259.4 (s, Ir–Cl) |
| 2b | 3241.2 (m, br) ~3290 (sh) | 3240.7 (m, br) | 3258.9 (s) 3102.1 287.1, 253.1 (s, Ir–Cl) |
| 2c | 3299.5 (m, br) ~3240 (sh) | 3281.6 (m, br) | 3279.3 (br) 290.8, 264.5 (s, Ir–Cl) |
| 2e | 3248.8 (m, br) ~3290 (sh) | 3267.4 (m, br) | nd |
| 2e-(¹⁵N)₂ | 3238.1 (m, br) ~3290 (sh) | 3260.1 (m, br) | nd |
| 3a | ~3230 (m, very br) ^{c,d} 2131.0 (s, Ir–H) | 3388.1 (m, br) ^c ~3223 (w, very br) 2130.2 (s, Ir–H) | 3313.4 (br) 2159.2 and 2140.0 (Ir–H) 282.0 (s, Ir–Cl) |
| 3b | 3201.9 (m, br) 2102.9 (s, Ir–H) | 3203.2 (m, br) 2097.2 (s, Ir–H) | 3257.0 (m, br) 2137.1 (s, Ir–H) 285.2 (s, Ir–Cl) |
| 3c | 3240.9 (m, br) 2099.7 (s, Ir–H) | 3251.1 (m, br) 2091.6 (s, Ir–H) | 3221.9 (br) 2090.8 (br, Ir–H) 283.4 (s, Ir–Cl) |
| 3d | nd | 2137.5 (s, Ir–H) ^c | 2142.5 and 2104.6 281.5 (s, Ir–Cl) |
| 3e-(¹⁵N)₂ | 3188.8 (m, br) ~3240 (shoulder) 2104.5 (s, Ir–H) | 3191.4 (m, br) ~3240 (shoulder) 2103.6 (s, Ir–H) | nd |
| 4b | 3384.4 (m) 2107.4 (s, Ir–H) | 3381.3 (m) 2104.8 (s, Ir–H) | 3227.0 (br) 2183.1 and 2111.3 (Ir–H) |
| 4d | 2120.4 (s, Ir–H) ^{c,d} | 2116.6 (s, Ir–H) ^{c,d} | nd |
| 4e-(¹⁵N)₂ | 3382.4 (m) 2102.4 (s, Ir–H) | 3379.6 (m) 2107.3 (s, Ir–H) | nd |
| 5a | nd | 3405.9 (m, br) | nd |
| 5b | nd | 3407.0 (m, br) | nd |

^a Solution samples measured in CaF₂ cells unless otherwise specified. ^b Measured as 3484.4 cm⁻¹ in NaCl cells. ^c Value measured on solution in NaCl cells. ^d In C₆D₆.

where the free ligands absorbed. This would indicate weaker hydrogen bonding, consistent with solid-state data on **3e-(¹⁵N)₂** and calculations below.

The wider spectral window afforded by the ATR instrument allowed one to observe bands for Ir–Cl stretches. As expected, the dichloro complexes showed two bands (in the ranges of 253.1–264.5 and 287.1–291.3 cm⁻¹), whereas the hydride chloride complexes showed only one (in the narrower range of 281.5–285.2 cm⁻¹). Significantly, the data for **3d** were in the same narrow range as the data for the other complexes with imidazolyl substituents, which would suggest that in complexes **3a–3c** the Ir–Cl bond is relatively unperturbed by hydrogen bonding in the solid state, consistent with the X-ray structure of **3b**.⁷⁹

Observation of Ir–H stretches was possible both in solution and in ATR samples. In the latter case, for some reason, two bands were seen even for the monohydride complexes **3**. Therefore, greater attention is paid to solution-phase spectra, where single strong bands for Ir–H absorption were seen. Only a single band was seen for dihydride **4b**, as well; we note that

many others have reported a single absorption for other Cp*Ir(H)₂(PR₃) complexes,^{80,81} and others have discussed why only one absorption might be seen for other metal dihydride species.¹⁵ Changing the R groups on P can easily change the Ir–H stretching frequency by more than 10 cm⁻¹,^{80,81} whereas previous work from our lab^{10–12,61,82} has shown that imidazol-2-yl and phenyl groups are electronically very similar and therefore should have little effect. A change in the value of $\nu_{\text{Ir-H}}$ from 2137.5 (**3d**) to 2091.6 cm⁻¹ (**3c**) suggests dihydrogen bonding in the latter species,²⁹ contradicting other evidence in this study. More compelling are the very similar $\nu_{\text{Ir-H}}$ values for **4b**, **4d**, and **4e-(¹⁵N)₂**, which are all within 12 cm⁻¹ of each other.

Catalysis. Three complexes were compared as catalysts for base-promoted transfer hydrogenation of acetophenone using *i*-PrOH; results are shown in Table 5. Conditions used were modeled after those reported elsewhere.^{83,84} Phosphine-free complex [Cp*IrCl(μ -Cl)]₂ was reasonably efficient, completing

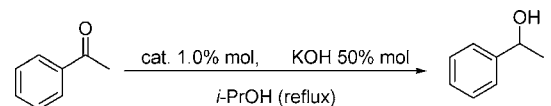
(79) For example, hydrogen bonding to Cl of (H)(Cl)Os(CO)(PR₃)₂ caused the Os–Cl stretching frequency to decrease from 398 to 378 cm⁻¹, whereas the Os–H and C–O stretching frequencies increased by 11–16 cm⁻¹. Yandulov, D. V.; Caulton, K. G.; Belkova, N. V.; Shubina, E. S.; Epstein, L. M.; Khoroshun, D. V.; Musaev, D. G.; Morokuma, K. *J. Am. Chem. Soc.* **1998**, *120*, 12553.

(80) Janowicz, A. H.; Bergman, R. G. *J. Am. Chem. Soc.* **1983**, *105*, 3929–3939.

(81) Paisner, S. N.; Burger, P.; Bergman, R. G. *Organometallics* **2000**, *19*, 2073–2083.

(82) Grotjahn, D. B.; Zeng, X.; Cooksy, A. L.; Kassel, W. S.; DiPasquale, A. G.; Zakharov, L. N.; Rheingold, A. L. *Organometallics* **2008**, *27*, 3626.

(83) Miecznikowski, J. R.; Crabtree, R. H. *Organometallics* **2004**, *23*, 629–631.

Table 5. Yields (%) of Transfer Hydrogenation of Acetophenone Using Three Catalysts^a


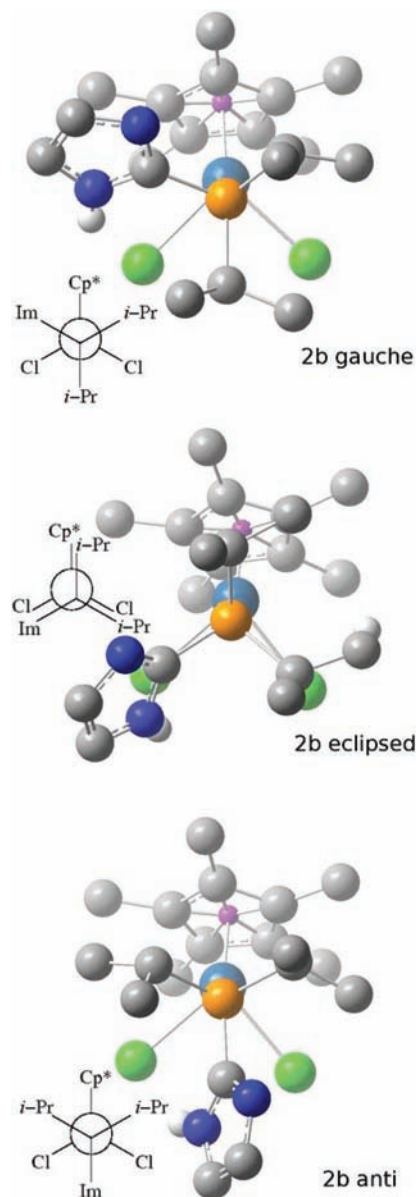
| time (h) | Catalyst | | |
|----------|-----------|---|-----------|
| | 2b | $[\text{Cp}^*\text{IrCl}(\mu\text{-Cl})_2]$ | 2d |
| 1 | 3.9 | 7.8 | 0 |
| 2 | 32.0 | | |
| 4 | 41.3 | 11.9 | 12.8 |
| 6 | 93.3 | | |
| 7 | >97.0 | | |
| 8 | | 83.9 | 24.7 |
| 24 | | >97.0 | 49.6 |

^a Reaction conditions: refluxing *i*-PrOH, substrate/Ir/KOH = 100:1:50, 0.1 M substrate in *i*-PrOH. Yields were determined by ¹H NMR spectroscopy (CDCl₃).

reduction within 24 h. The complex made using a non-heterocyclic phosphine (**2d**) was approximately 2–4 times slower, whereas the analogue **2b** was about 3 times faster. Additional experiments would be needed to elucidate the mechanistic reasons for acceleration provided by the NH phosphine, which is somewhat modest. However, under the basic conditions employed, one can imagine that the NH may be deprotonated and the resulting pendant base may assist in one or more steps of the transfer hydrogenation, for example, by deprotonating the alcohol as it binds to the metal and forms an alkoxide, several examples of which are known on Cp*Ir fragments.^{85–87}

Calculations. Computational modeling of several complexes was carried out using Gaussian 03⁸⁸ in order to provide a theoretical basis for some of the observations. Unless indicated otherwise, all calculations were carried out using the B3LYP density functional method^{89,90} and Dunning's cc-pVDZ basis set⁹¹ for the main group atoms and the CEP-121G basis set of Stevens et al.⁹² for the Ir. The conformations of the *i*-Pr groups were not rigorously surveyed but are consistent among the structures tabulated here. Tests of several **3b** structures suggest that the *i*-Pr conformations impact the calculated energies by 2 kcal/mol or less.

A survey of the conformations in **2**, **3**, and **4** consistently predicts that *endo*-NH–Cl hydrogen-bonded structures are stabilized by free energies of 10 to 12 kcal/mol, while *endo*-NH–H structures are stabilized by 6–7 kcal/mol, in comparison to *exo* structures with the NH oriented away from the other ligands (Table 6). Furthermore, each NH–Cl structure has two distinct conformations, *anti* and *gauche* (with respect to rotation about the Ir–P bond, Figure 8). In **2** and **3**, the *anti* is always

**Figure 8.** Optimized *gauche*, eclipsed (transition state), and *anti* conformations of **2b**. All hydrogens but the NH atom are omitted for clarity.

higher in energy, but by less than 2.5 kcal/mol. In contrast, for the *endo* geometries of **4**, only the *anti* was found to be stable.

Table 6. Relative B3LYP/cc-pVDZ, CEP-121G Free Energies (kcal/mol) of Selected Conformers

| Species | <i>endo</i> H..Cl | | | <i>exo</i> <i>gauche</i> |
|-----------|-------------------|------------------|------------------|-----------------------------|
| | <i>gauche</i> | eclipsed (TS) | <i>anti</i> | |
| 2b | 0.0 | 14.1 | 2.2 | 12.5 |
| 2c | 0.0 | 11.8 | 2.2 | 10.4 |
| 2e | 0.0 | 15.3 | 1.2 | 11.8 |
| | <i>endo</i> H..Cl | | <i>endo</i> H..H | <i>exo</i> |
| | <i>gauche</i> | <i>anti</i> | <i>gauche</i> | <i>gauche</i> |
| 3b | 0.0 | 0.5 | 7.4 | 12.3 |
| 3e | 0.0 | 1.1 | 6.5 | 12.3 |
| | <i>endo</i> H..H | | | <i>exo</i> |
| | <i>anti</i> | | | <i>gauche</i> |
| 4b | 0.0 | | | 5.8 |
| 4e | 0.0 | | | 7.4 |

- (84) Corberán, R.; Sanaú, M.; Peris, E. *Organometallics* **2007**, *26*, 3492–3498.
- (85) Newman, L. J.; Bergman, R. G. *J. Am. Chem. Soc.* **1985**, *107*, 5314–5315.
- (86) Ritter, J. C. M.; Bergman, R. G. *J. Am. Chem. Soc.* **1998**, *120*, 6826–6827.
- (87) Glueck, D. S.; Winslow, L. J. N.; Bergman, R. G. *Organometallics* **1991**, *10*, 1462–1479.
- (88) Frisch, M. J.; et al. *Gaussian 03*; Gaussian, Inc.: Wallingford, CT, 2004.
- (89) Becke, A. D. *J. Chem. Phys.* **1993**, *98*, 5648–5652.
- (90) Lee, C.; Yang, W.; Parr, R. G. *Phys. Rev. B* **1988**, *37*, 785–789.
- (91) Dunning, J. T. H. *J. Chem. Phys.* **1989**, *90*, 1007–1023.
- (92) Stevens, W. J.; Krauss, M.; Basch, H.; Jasien, P. G. *Can. J. Chem.* **1992**, *70*, 612–630.

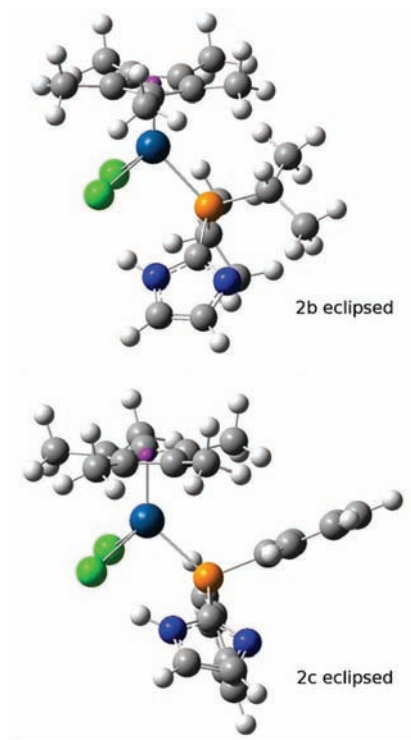


Figure 9. Eclipsed conformations of **2b** and **2c**, optimized geometries as transition states between *gauche* and *anti* conformations, showing the greater steric interaction in the **2b** transition state.

In all cases, the energy ordering of the *gauche* and *anti* conformers may be predicted on the basis of steric interactions with the Cp* group. The more stable conformer has the largest minimum distance between atoms on the Cp* and on the phosphine R groups.

By this reasoning, the *gauche* conformers are favored by **2** and **3** because the P–Ir–Cp* angle decreases by about 7° on replacement of the H atoms in **4** by Cl atoms. This increases the importance of Cp* steric interactions with the R groups of the phosphine in **2** and **3**. It is then more favorable to place a flat imidazole near the Cp* ring, rotated so its plane is roughly parallel to the Cp*, than an *i*-Pr with hydrogens sticking out in several directions. We emphasize, however, that other steric interactions, as between the phosphine R groups themselves, are expected to play a role in these energetics, and these dependencies have not been rigorously tested. Furthermore, the predicted energy differences between the *gauche* and *anti* conformers are comparable to the expected error of the calculations.

Only *gauche* appears to be stable for the *exo* geometries, perhaps because in this conformation the rotation of the imidazole to the *endo* form is hindered by the Cp*. In **2**, with two chlorides, the *endo-anti* conformer effectively has *C_s* symmetry, assuming rapid motion across the calculated barrier of 1.4 kcal/mol for rotating the NH from one Cl to the other.

To better characterize the conformational dynamics of **2**, the transition states between the *anti* and *gauche* forms were optimized. As expected, the transition states correspond to eclipsed conformations (Figure 9), and the activation barriers are dominated by the steric interaction between the Cp* and the R group on the phosphine. For **2b** and **2e**, the two R groups are isopropyls, which align roughly parallel to each other to minimize their steric interaction with each other.

Table 7. Experimental and Calculated Properties of the N–H Bonds in **1e**, **3e**, and **4e**

| species | $^1J_{\text{NH}}$ (exp) (Hz) | $^1J_{\text{NH}}$ (calcd) (Hz) | r_{NH} (Å) |
|-----------|------------------------------|--------------------------------|---------------------|
| 1e | 93.5 | 92.0 | 1.013 |
| 3e | 95.1 | 92.6 | 1.026 |
| 4e | 95.3 | 94.0 | 1.017 |

As a result, the isopropyls are aligned roughly perpendicular to the Cp* plane at the eclipsed transition state, and distances as small as 2.1 Å occur between atoms of the Cp* and atoms of the *i*-Pr groups. In contrast, the corresponding interaction in the transition state for **2c** places a flat phenyl group roughly parallel to the Cp* plane, and minimum distances between the two groups are at least 2.7 Å. As a result, the free energy of activation from *anti* to *gauche* is predicted to be 11.8 kcal/mol for **2c** but 14.1 and 15.3 kcal/mol for **2b** and **2e**, respectively.

The ^{15}N – ^1H *J* couplings in **1e**, **3e**, and **4e** were predicted using the GIAO approximation. Although the calculated values uniformly underestimate the coupling constant, they correctly reproduce the observed ordering of the values (Table 7), with both **3e** and **4e** having larger couplings than **1e**, despite the lengthening of their N–H bonds by hydrogen bonding to the neighboring Cl. Interestingly, the major contributor to the increase in $^1J_{\text{NH}}$ from **1e** to **3e** and **4e** is the Fermi contact term, yet the s character of the orbitals centered at the N and H atoms decreases as this bond stretches. The increase in $^1J_{\text{NH}}$ appears to be caused by the small, added electron density at the N and H atoms donated by the Cl at the other end of the hydrogen bond. A comparable increase in $^1J_{\text{NH}}$ (0.4–0.6 Hz) is predicted for imidazole when a HCl molecule is placed at Cl–N separations of 3.0–3.4 Å.

Four initial geometries of **3b**, including the X-ray structure, were constructed specifically to test the viability of the NH–hydride interaction indicated by the X-ray structure. Upon optimizing these geometries, the only one of these structures to maintain the NH–hydride bond has the imidazole placed in a *gauche* conformation, such that the Cl atom is unavailable for hydrogen bonding. All others converged to either the *endo-gauche* or *endo-anti* with hydrogen bonding to the chloride. Extending the basis set on the interacting atoms to include diffuse functions failed to make the NH–hydride conformation more stable than the NH–Cl, as did replacing the DFT calculations by a much more demanding CISD method.⁹³

Conclusions

All imidazolylphosphine complexes in this study show evidence of hydrogen bonding involving the NH, as evidenced by a combination of data. In all solvents examined and at all temperatures, all monohydride [**3a–3c**, **3e**-(^{15}N)₂] and dihydride [**4b**, **4e**-(^{15}N)₂] complexes with an imidazolyl group appeared as a single species in ^1H , ^{31}P , ^{13}C , and ^{15}N NMR spectra. Meanwhile, dichloride complex **2c** gave evidence of only one species, whereas **2a**, **2b**, and **2e** showed evidence of more than one species, all involving hydrogen bonding, but with distinct differences. Examination of crystal structures and DFT calculations both point to the existence of two low-lying conformers, each defined as *endo* because hydrogen bonding of the NH to chloride (**2**, **3**) or hydride (**4**) is stabilizing. The two conformers are defined as *anti* and *gauche*, using the relationship of the Cp* and imidazolyl substituents on Ir and P as reference.

(93) Raghavachari, K.; Pople, J. A. *Int. J. Quantum Chem.* **1981**, *20*, 1067–1071.

Significantly, for complexes with isopropyl groups on P, low-temperature NMR spectra could be used to identify the *anti* and *gauche* conformers on the basis of symmetry.

Several lines of evidence (supported by DFT calculations) point to stronger hydrogen bonding to chloride than hydride in this system, which stands in distinct contrast to another Ir(III) system studied previously.¹⁷ Significantly, the X-ray diffraction structure of **3e**-(¹⁵N)₂, showing hydrogen bonding to chloride rather than hydride, differs from that of less hindered analogue **3b** because competing intermolecular hydrogen bonding is suppressed. Infrared data for NH stretching show greater changes from free ligand values when at least one chloride ligand is present in the coordination sphere.

For **2a**, NMR data, particularly ¹⁵N chemical shift information, point to ionization of chloride in chlorinated solvents, nitromethane, or isopropyl alcohol, forming chelate **5a-Cl** (hypothesis C), a result also seen on addition of protic solute HOCH₂CF₃ to a toluene solution of **2a**. In comparison, in either benzene or toluene, **2a** exists as one conformer. In contrast, for **2b**, strong evidence was found for the presence of *anti* and *gauche* conformers (hypothesis B) in solution. Low-temperature NMR data involving ¹H, ¹³C, ³¹P, and, where available, ¹⁵N in **2b** and its analogues **2e** and **2e**-(¹⁵N)₂ are completely consistent with calculations. The difference between **2a** and **2b**, which are homologues, is striking and points to the importance of innocent ligand substituents in determining the behavior of hemilabile and bifunctional systems. Finally, imidazolylphosphine complex **2b** was somewhat more effective as a transfer hydrogenation catalyst than non-heterocyclic control compound

2d. Imidazolylphosphines with a free NH promise to be the subject of additional structural and catalytic studies because of their unusual ability to either accept or donate a hydrogen bond, thereby affecting catalytic turnover and performance.

The structural studies highlighting the difference between **2a** and **2b** show how relying on a single kind of spectroscopic evidence (IR, ¹H, ¹³C, or ¹⁵N NMR) to characterize hydrogen bonding can be very risky, even when seemingly similar species are compared.

Acknowledgment. The NSF is thanked for support of the research done for this project at San Diego State University under CHE 0415783 and CHE 0719575, and for travel support under INT 0128861. H.A. would like to thank UPMC-Paris 6 for travel support under ongoing collaboration (DRI) between SDSU and UPMC-Paris 6. S.C.-L. thanks Fulbright for an award funding her stay at San Diego State University.

Supporting Information Available: Preparative details for all compounds, graphical representations of 2D NMR data used in compiling Tables 3 and 4, the molecular structure of **2a** (Figure S1), ¹H NMR spectrum of **2e**-(¹⁵N)₂ (Figure S2) showing peaks for *anti* and *gauche* conformers, crystallographic data and details for X-ray diffraction studies, CIF files for all structures, tables for DFT calculations of structures, energies, IR and NMR data, and complete ref 88. This material is available free of charge via the Internet at <http://pubs.acs.org>.

JA906712G